

Utility of dissolved Barium in distinguishing North American from Eurasian runoff in the Arctic Ocean

T. Roeske^{1*}, D. Bauch², M. Rutgers v. d. Loeff¹, B. Rabe¹

¹Alfred Wegener Institut für Polar- und Meeresforschung (AWI)

² Leibniz Institut für Meereswissenschaften an der Universität Kiel (IFM-GEOMAR)

*Corresponding author:

Tobias Roeske c/o Michiel Rutgers van der Loeff
Alfred Wegener Institute for Polar and Marine Research (AWI)
Am Handelshafen 12
27570 Bremerhaven, Germany
E-Mail: tobias.roeske@awi.de
Phone: +49 471 4831 1259
Fax: +49 471 4831 1425

Abstract

Dissolved barium has been shown to have the potential to distinguish Eurasian from North American (NA) river runoff. As part of the ARK-XXII/2 Polarstern expedition in summer 2007, Ba was analyzed in the Barents, Kara, Laptev seas, and the Eurasian Basins as well as the Makarov Basin up to the Alpha and Mendeleev Ridges. By combining salinity, $\delta^{18}\text{O}$ and initial phosphate corrected for mineralization with oxygen (PO_4^*) or N/P ratios we identified the water mass fractions of meteoric water, sea ice meltwater, and marine waters of Atlantic as well as Pacific origin in the upper water column. In all basins inside the lower halocline layer and the Arctic intermediate waters we find Ba concentrations close to those of the Fram Strait branch of the lower halocline (41-45 nM), reflecting the composition of the incoming Atlantic water. A layer of upper halocline water (UHW) with higher Ba concentrations (45-55 nM) is identified in the Makarov Basin. Atop of the UHW, the Surface Mixed Layer (SML), including the summer and winter mixed layers, has high concentrations of Ba (58-67 nM). In the SML of the investigated area of the central Arctic the meteoric fraction can be identified by assuming a conservative behavior of Ba to be primarily of Eurasian river origin. However, in productive coastal regions biological removal compromises the use of Ba to distinguish between Eurasian and NA rivers. As a consequence, the NA river water fraction is underestimated in productive surface waters or waters that have passed a productive region, whereas this fraction is overestimated in subsurface waters containing remineralised Ba, particularly when these waters have passed productive shelf regions. Especially in the Laptev Sea and small regions in the Barents Sea, Ba concentrations are low in surface waters. In the Laptev Sea exceptionally high Ba concentrations in shelf bottom waters indicate that Ba is removed from surface waters to deep waters by biological activity enhanced by increasing ice-free conditions as well as by scavenging by organic matter of terrestrial origin. We interpret high Ba concentrations in the UHW of the Makarov Basin to result from enrichment by remineralisation in bottom waters on the shelf of the Chukchi Sea and therefore the calculated NA runoff is an artefact. We conclude that no NA runoff can be demonstrated unequivocally anywhere during our expedition with the set of tracers considered here. Small contributions of NA runoff may have been masked by Ba depletion and could only be resolved by supportive tracers on the uptake history. We thus suggest that Ba has to be used with care as it can put limits but not yield quantitative water mass distributions. Only if the extra Ba inputs exceed the cumulative biological uptake the signal can be unequivocally attributed to NA runoff.

Keywords: Barium; Arctic Ocean; biological cycling; surface water; GEOTRACES

1 Introduction

The Arctic Ocean covers an area $9.6 \cdot 10^6 \text{ km}^2$ (Serreze et al., 2006) corresponding to 5 % of the world oceans while it constitutes only 1.5 % in volume (Guay and Falkner, 1998a). The shelves make out more than one third of this area. About 10 % of the world's river discharge flows into the Arctic Ocean making it one of the most important estuarine systems (Aagaard and Carmack, 1989; Dickson et al., 2007). These rivers contribute to the fresh surface layer of the Arctic Ocean. Some part of the water from the Ob and Yenisey rivers enters the Laptev Sea through Wilkitsky Strait and merges with waters from the Lena River. This coastal current water is partly reflected northwards into the Canadian Basins in the East Siberian Sea (Guay et al., 2001). The Surface (summer) Mixed Layer (SML) in the Arctic Ocean is underlain by a winter mixed layer, with temperatures close to the freezing point of seawater, which in turn is overlying a thick halocline layer (Aagaard et al., 1981). The halocline is formed by local convective mixing and is also maintained by waters advected from the shelf seas. On the Canadian side of the Lomonosov Ridge a layer of upper halocline water (UHW) is characterized by a salinity of about 32.8 to 33.2 and a maximum in nutrients may be identified (Jones and Anderson, 1986; Morison et al., 1998). This UHW is partly composed of Pacific waters of winter origin which tend to enter the interior Arctic below the upper mixed layer because they are generally more saline (Coachman and Shigaev, 1992; Weingartner et al., 1998). Beneath the UHW a layer of lower halocline water (LHW) with salinity ranging from 34.2 to 34.4 has been identified (Jones and Anderson, 1986). These waters of Atlantic origin are divided further into a Barents Sea branch halocline and a Fram Strait branch halocline (Rudels et al., 2004). Below the halocline are a layer of Atlantic and Arctic intermediate waters as well as deep and bottom waters.

The marine biogeochemical behavior of Ba is described in detail in Falkner et al. (1993; 1994). Usually, dissolved Ba is linked closely to hard-part nutrients as alkalinity (reflecting CaCO_3) and Si, showing depletion in oceanic surface waters and enrichment in deep waters and along advective flow-lines (Chan et al., 1977; Falkner et al., 1993; Lea and Boyle, 1990). This distribution is primarily ascribed to the uptake of Ba in surface waters. As the mineral barite is being formed in microenvironments in intermediate waters, Ba is removed from the dissolved phase at these depths, sinking with fecal pellets and regenerates from the sediment (Bishop, 1988; Collier and Edmond, 1984; Dehairs et al., 1980; Dymond et al., 1992; Falkner et al., 1994; Guay and Falkner, 1998b). Barite formation may involve remineralization of acantharians which accumulate Ba in their SrSO_4 skeleton (Bernstein et al., 1992; Bernstein et al., 1998). Furthermore barite formation is induced by diatoms accumulating Ba (Esser and Volpe, 2002). Rivers and hydrothermal venting are the main sources of Ba to the oceans (Edmond et al., 1979; Guay and Falkner, 1998a; Martin and Meybeck, 1979; Von Damm et al., 1985). Most hydrothermal Ba is thought to precipitate inorganically as barite in the vicinity of hot spring sources (Von Damm, 1990). In estuaries Ba is enriched by desorption from river-borne clays in exchange with the more abundant cations of seawater (Carroll et al., 1993; Falkner et al., 1993; Hanor and Chan, 1977; Li and Chan, 1979). Ba is highly enriched in North American (NA) rivers (Mackenzie) with respect to Eurasian rivers and typical Atlantic and Pacific surface waters (Cooper et al., 2008; Guay and Falkner, 1998b; Taylor et al., 2003).

The strong salinity gradients between the different water masses result in a strong stratification especially in the Arctic Ocean surface layer. This is essential for the formation of sea ice and biological productivity in the ice-free areas. The largest freshwater inventory is found in the upper 300 m of the Canadian Basin (Rabe et al., 2009; Rabe et al., 2011; Yamamoto-Kawai et al., 2008). These waters are composed of Eurasian and NA river runoff, Pacific water modified in the Chukchi Sea, sea ice melt and net precipitation, insulating sea ice from the heat in the relatively warm Atlantic waters underneath (Björk and Söderkvist, 2002; Shimada et al., 2005). With its positive buoyancy this freshwater is one of the factors governing the formation of convective deep water in the North Atlantic and thus are of importance for the global ocean circulation and climate (Aagaard and Carmack, 1989; Guay et al., 2009). Based on salinity and oxygen isotopes, fractions of meteoric water, sea ice melt, and high salinity marine water may be discerned in surface waters (Bauch et al., 1995). The high salinity fraction can be divided in Atlantic and Pacific fractions by using initial phosphate corrected for mineralization with oxygen (PO_4^*) (Broecker, 1985; Ekwurzel et al., 2001). Alternatively N/P ratios can be used to identify fractions of Atlantic or Pacific origin (Yamamoto-Kawai et al., 2008; Bauch et al., 2011a). Dissolved Ba was described previously as a powerful quasi-conservative tracer for Arctic water masses (Falkner et al., 1994; Guay and Falkner, 1998b; Taylor et al., 2003). This is true especially in the UHW (< 200 m) and the SML of the Arctic Ocean where NA runoff with high Ba content can be distinguished from Eurasian runoff. In combination with other tracers of freshwater components (e.g. salinity, $\delta^{18}\text{O}$, nutrients, ^{228}Ra , fluorescence) it provides information on the riverine sources of meteoric water. However, the inclusion of Ba in the biogeochemical cycling of organic material implies that changes in productivity may impact its use as (semi conservative) tracer. Indeed, Abrahamsen et al. (2009) suggest increasingly ice-free conditions to compromise the quantitative use of barium as a tracer of river water in the Arctic Ocean. This is strengthened by observations that Ba is released at depth from particles convecting down at the shelves' slopes, thus showing that biological uptake is of importance for its redistribution (Roeske et al., submitted).

In recent years, Arctic sea ice decline has risen from 2.2 to 3 % per decade in 1979-1996 to about 10 % in the last ten years (Comiso et al., 2008). Large areas especially on the shelves are free of sea ice for a prolonged time and the change in summer sea ice cover from 2006-2007, according to a model by Arrigo et al. (2008), may have caused an increase in primary production by $35 \text{ Tg}\cdot\text{y}^{-1}$. This results in higher carbon export on the shelves and has influence on Ba concentrations and thus its conservative behavior in the Arctic Ocean. We thus investigate to what extent recent changes in the Arctic have an impact on the utility of dissolved Ba to distinguish NA from Eurasian runoff.

2 Methods

In a companion paper (Roeske et al., submitted) from the same expedition we describe full depth profiles together with dissolved aluminium and silicate excluding surface water, while here we concentrate on the surface layer. Water samples were collected during Polarstern expedition ARK-XXII/2 in summer of 2007. The sampled area reaches from the Barents Sea to the Nansen Basin to the Kara Sea and then to the Makarov Basin and finally the Laptev Sea (Schauer, 2008) (table 1, fig. 1). There were 38 vertical profiles with about 450 samples (of which 246 are surface samples, table 2) for Ba (Pangaea data repository at <http://doi.pangaea.de/10.1594/PANGAEA.758745>, Roeske et al., 2011), using an

ultra-clean Titanium-rosette with 12 L bottles from Royal NIOZ (De Baar et al., 2008). 15 ml LDPE bottles were used to collect samples for Ba. The bottles were pre-rinsed thrice with the water to be sampled. Unfiltered samples were acidified with 30 μ l quartz-distilled HCl and afterwards tightly sealed with parafilm and stored at room temperature. Samples from stations 228 through 246 were filtered onboard in a clean room container. In order to determine whether ultra-clean sampling is necessary for determination of Ba, parallel samples were taken on the entire depth profile using the conventional AWI rosette at station 266. A further set of filtered samples was analyzed in 2009 from samples archived by the NIOZ team.

Ba was analyzed using an isotope dilution procedure (Falkner et al., 1993; Guay and Falkner, 1998b; Klinkhammer and Chan, 1990) and then measured with a Thermo-Finnigan Element2 high resolution sector field inductively coupled plasma mass spectrometer (SF-ICP-MS). A ^{135}Ba -enriched solution (produced from BaCO_3 from Spex Industry) was calibrated using commercial ICP-MS standard solutions (Spetec® single element Ba for ICP-MS and NIST standard reference material® 1643e). Aliquots of 500 μ l were spiked with this ^{135}Ba -enriched solution to obtain a $^{138}\text{Ba}/^{135}\text{Ba}$ ratio between 0.7 to 1 to minimize error propagation (Klinkhammer and Chan, 1990) and diluted hundredfold using 18.2 M Ω water. Spiking and dilution were done gravimetrically. About 1 ml of the samples were introduced via autosampler (~200 μ l/min uptake) to a micro-concentric Teflon® nebulizer and an Apex® Q quartz desolvation chamber. The SF-ICP-MS was operated in peak jump mode and data were accumulated in three 20 s intervals for masses 135, 137, and 138. The SF-ICP-MS was operated in low resolution mode ($\Delta m \sim 300$). A three minute wash-out with 1 M double-distilled HNO_3 was followed by a 90 sec. take-up time to make memory effects negligible. A blank and a monitor for mass-bias correction (Canadian certified reference material CRM NASS-5) bracketed every five samples. In addition, in every tray of 19 samples at least two standards were included to check consistency. Random repeats of two samples were also done in each run. Samples were analyzed twice. If duplicates varied by more than the calculated maximum method error, samples were prepared and analyzed anew. Sensitivity of the SF-ICP-MS resulted in about 200000 cps ^{138}Ba in samples of Atlantic background. Blanks always were below 2000 cps being usually below 1000 cps.

At station 266 profiles were taken on both the ultra-clean and the normal rosette and Ba results were equal within errors (cf. Roeske et al., 2011). At station 352 positioned in the Makarov Basin multiple samples were taken at a depth of 2000 m for interlab analyses (with two labs taking part using ICP-MS, including ours; at one lab analyses were done by ICP-MS and ICP-OES; at a fourth lab analyses were done by TIMS). The labs used different standards as absolute references for their ^{135}Ba solution. We noticed that calibration of our ^{135}Ba standard solution with commercial ICP-MS standard solutions (Spetec® single element Ba for ICP-MS and NIST standard reference material® 1643e) resulted in a concentration 7.2 % higher than calibrations with the natural standard solutions SLRS-3 (Ba = 13.4 ± 0.6 $\mu\text{g/L}$), SLRS-4 (Ba = 12.2 ± 0.2 $\mu\text{g/L}$), SLRS-5 (Ba = 14.0 ± 0.5 $\mu\text{g/L}$), and OMP (Ba = 10.4 ± 0.2 $\mu\text{g/L}$, an inhouse standard prepared by C. Jeandel, LEGOS, Toulouse, France). The concentration was within errors of the other labs dependent on the method used for calibration. Using the commercial ICP-MS standards we were in agreement (within 0.9-5.5 %) with the lab also using a commercial ICP-MS standard on a TIMS. Using the natural waters we agreed (within 0.3-2.6 %) with the other two labs doing the same on ICP-MS and ICP-OES. An additional interlab comparison (two labs,

including ours) on samples of two different profiles resulted in correlations of 0.995 and 0.996 (R^2) and slopes of 0.977 and 0.994, respectively, also using natural waters as reference for the ^{135}Ba standard.

Taylor et al. (2003) discovered problems with the stoichiometry of the starting salts of commercial BaCO_3 standards and thus used archived GEOSECS standards. We thus compared our data below the halocline layer (least influenced by short term processes) to other data in our sample area of the same year (Abrahamsen, personal communication), plotting Ba against salinity (fig. 2). Abrahamsen et al. (2009), chosen here for reference, use the same procedure previously used for all published data in the Arctic (cf. Falkner et al., 1993; 1994; Guay and Falkner, 1998b; 1998; Taylor et al., 2003). We found the best match (fig. 2) when using commercial standards. In order to keep in line with existing literature we decided to adopt that calibration procedure for the present study.

Ba concentrations were calculated following Klinkhammer and Chan (1990):

$$[\text{Ba}](\text{nmol} \cdot \text{g}^{-1}) = \frac{(R_m - R_{spk})[^{135}\text{Ba}]W_{spk}}{\left(1 - \frac{R_m}{R_{nat}}\right)A_{138}W_{sam}} \quad (1)$$

where R_m = ratio measured, R_{nat} = the naturally occurring $^{138}\text{Ba}/^{135}\text{Ba}$ mass ratio ($R_{nat} = 10.877$), $^{138}\text{Ba}/^{135}\text{Ba}$ = ratio of the spike ($R_{spk} = 0.025$), ^{135}Ba = the concentration of ^{135}Ba in the spike solution ($[^{135}\text{Ba}] = 9.04$ ppb and 9.53 ppb in 2008 and 2009 respectively), A_{138} = the natural abundance of ^{138}Ba ($A_{138} = 0.7166$) and W_{sam} and W_{spk} = the weights of the sample and the spike respectively.

Mass discrimination, called "mass bias", is derived by a method used by Freydier et al. (1995) by measuring the masses 135, 137, and 138 of a natural Ba solution (Canadian CRM NASS-5). It follows a linear law following eqn. 2:

$$R_m = R_t(1 + n\alpha) \quad (2)$$

where R_m = measured isotopic ratio, R_t = true value of this isotopic ratio, n = number of mass units between the two isotopes, and α = unitary mass discrimination. The recommended point and discrimination line are also given by Freydier et al. (1995).

Calculated maximum error of the method always was below 3 %. Precision of repeated analyses of samples and standard solutions was always within 1.5 % ($1-\sigma$). The error of the ratio $^{138}\text{Ba}/^{135}\text{Ba}$ was 0.6 % or better.

Salinity (conductivity), temperature and depth (pressure) were measured on two CTD's, one from the Netherlands Institute for Sea Research (NIOZ) and one from the Alfred Wegener Institute for Polar and Marine Research (AWI), Germany. Both were Sea Bird electronics and calibrated onboard (Schauer, 2008).

Water samples for stable oxygen isotope analysis were taken both with the ultra-clean Titanium-rosette from Royal NIOZ as well as with the conventional AWI rosette. Oxygen isotopes were analyzed at the Leibniz Laboratory (Kiel, Germany) applying the CO_2 - water isotope equilibration technique on at least 2 sub-samples on a Finnigan gas bench II unit coupled to a Finnigan DeltaPlusXL. The overall measurement precision for all $\delta^{18}\text{O}$ analysis is ± 0.03 ‰ or smaller. The $^{18}\text{O}/^{16}\text{O}$ ratio is given versus VSMOW in the usual δ -notation (Craig, 1961).

Figures were created using the Ocean Data View software (Schlitzer, 2010).

3 Results

All Ba data are presented in table 2 and are also available on the Pangaea data base (Roeske et al., 2011). An overview of the elemental dissolved Ba distribution in the surface water layer of the sections is seen in figures 3-7a. Additional panels on water mass fractions together with T_{pot} and salinity are displayed in Bauch et al. (2011a). Potential temperature and salinity data are courtesy of the oceanography group of ARKXXII/2 (Schauer, 2008). Ba concentrations of Atlantic origin, ranging from 41 to 45 nM, are characteristic throughout the investigated area (figs. 3-7a), especially inside of the LHW. Shelf bottom waters of the Laptev Sea have concentrations up to 96.6 nM (fig. 7a), and in surface waters atop the UHW concentrations increase to 67 nM towards the Canada Basin (fig. 5a). Concentrations lower than 40 nM are found predominantly in surface waters of the Barents Sea. In surface waters of the Laptev Sea as well as in the Barents Sea at about 80°N low concentrations of 37.9 to 38.8 nM and 30.3 to 31 nM respectively are seen (figs. 3a & 7a).

The depth of the upper mixed layer was determined by density gradient from temperature and salinity profiles of 40 stations from July to September 2007. The total expedition included 185 stations, but only the stations where Ba data is available were considered. The SML is between 8 and 32 m thick, separated from underlying waters by a steep salinity gradient. A discontinuity and/ or gradient in the profiles of temperature and oxygen often coincided with the salinity gradient. Typical salinities in the SML range from about 27 to 31 on the Canadian side of the Lomonosov Ridge, 31 to 34 in the Eurasian Basins, 32 to 35 in the Barents Sea, and 29 to 33 in the Laptev Sea. Following Guay and Falkner (1998b) the UHW is defined by salinities from 32.5 to 33.5 and a nutrient maximum, while the LHW is taken to be the layer of salinities of 34 to 34.5 and a NO minimum. The UHW was found at a depth of 50 to 120 m and has a maximal thickness of 20 m. In this layer Ba concentrations from 45.3 to 54.8 nM are observed, close to Ba values found within this layer by Guay and Falkner (1998b). The LHW has a thickness of 20 to 100 m and can be traced over the whole area investigated at depths from 0 to 175 m. Concentrations of Ba ranging from 41 to 47.7 nM are found in the LHW. Guay and Falkner (1998b) found concentrations < 46 nM in this layer. We found highest concentrations in the Canadian Basin and at station 400 at the Laptev Sea slope as well as one exceptionally high concentration of 51.6 nM at station 385 in 100 m depth.

3.1 Balancing the fresh water fraction in the upper water column

The water mass fractions are calculated using a four-component system of mass balance equations based on salinity, $\delta^{18}O$, and PO_4^* , a quasi-conservative tracer based on phosphate and dissolved oxygen (Broecker, 1985), using a method similar to that of Ekwurzel et al. (2001):

$$f_a + f_p + f_i + f_r = 1 \quad (3)$$

$$f_a S_a + f_p S_p + f_i S_i + f_r S_r = S \quad (4)$$

$$f_a \delta^{18}O_a + f_p \delta^{18}O_p + f_i \delta^{18}O_i + f_r \delta^{18}O_r = \delta^{18}O \quad (5)$$

$$f_a PO_{4a}^* + f_p PO_{4p}^* + f_i PO_{4i}^* + f_r PO_{4r}^* = PO_4^* \quad (6)$$

where f_a is the Atlantic water fraction, f_p is Pacific water, f_i is sea ice melt (or ice formation if negative), and f_r is meteoric water (neglecting precipitation this is river water). For further details on the fraction calculation refer also to Bauch et al. (2011a). If the resulting fraction of Pacific water is negative (because of vanishingly small quantities of Pacific water combined with small inaccuracies in end-members

and measurements), a three-component system of equations is solved instead, only using eqns. 3 to 5 with f_p set to zero (Östlund and Hut, 1984). Our end-members are following Ekwurzel et al. (2001) (table 3). The endmember for meteoric water is set to a $\delta^{18}\text{O}$ of -20‰ reflecting average meteoric waters in the Arctic Ocean (Bauch et al., 2010). Calculation of PO_4^* by dissolved O_2 is done assuming that the water is not in exchange with the atmosphere. While this is largely true under the winter sea ice cover, the Arctic Ocean is partly free of sea ice in summer and ice-free areas were especially large in summer 2007. Exchange of dissolved O_2 with the atmosphere may lead to an underestimation of f_p in the summer mixed layer (Bauch et al., 2011a). Bauch et al. (2011a) thus additionally follow the procedure based on N/P presented by Jones et al. (1998; 2008) and Yamamoto-Kawai et al. (2008) using the “pure Pacific water” correlation line $[\text{NO}_x] = 15.314 \cdot [\text{PO}_4] - 14.395$ (Jones et al., 2008) and an adjusted “pure Atlantic water” correlation line (Bauch et al., 2011a) $[\text{NO}_x] = 16.785 \cdot [\text{PO}_4] - 1.9126$. On the other hand denitrification creates an apparent f_p signal and Bauch et al. (2011a) use the brine signal (negative f_i) to identify this apparent f_p within the Transpolar Drift. They conclude that within errors of the method, the N/P-based f_p signal observed at stations over the Lomonosov Ridge is entirely caused by denitrification on the Siberian shelves and is therefore an apparent f_p signal. The N/P-based method is therefore used on the Canadian side of the Lomonosov Ridge only while over the Ridge and in the Eurasian Basin we use the PO_4^* -based method.

We find varying fractions of meteoric water in the SML (figs. 3-7b, 6c). Largest f_r within the Arctic Ocean basins with up to 19 % are found in the Makarov Basin. In the Laptev Sea f_r reaches 16 % at our southernmost position and in sections A and B in the western part of the Eurasian Basin we find only up to 3 % (see fig. 8b for integrated river water in the upper 50 m). Sea ice meltwater and sea ice formation (negative fractions of sea ice meltwater) in the upper 50 m are shown in fig. 8d. While in the central Arctic Ocean net sea ice formation is dominant, in the western part of the Eurasian Basin close to the shelves we find large areas of net sea ice melt. Pacific waters are found to the east of 150°E only (fig. 8c).

Because of the distinct end-member Ba concentrations of the NA and Eurasian river inputs to the Arctic Ocean (Falkner et al., 1994; Guay and Falkner, 1998b), and assuming in a first approximation a conservative behaviour of Ba we are able to solve a further system of mass balance equations (Guay et al., 2009):

$$f_E + f_N = f_r \quad (7)$$

$$f_i Ba_i + f_s Ba_s + f_E Ba_E + f_N Ba_N = Ba \quad (8)$$

$$\frac{f_p}{f_a + f_p} Ba_p + \frac{f_a}{f_a + f_p} Ba_a = Ba_s \quad (9)$$

where f_s is the high-salinity water (Atlantic and Pacific) and f_E and f_N are the Eurasian and NA river runoff respectively. This allows us to distinguish Eurasian from NA runoff. We used end-member Ba concentrations by Guay et al. (2009) except for the Atlantic end-member, which is chosen from the core of the Atlantic water in the Nansen Basin of section A (see section 2, table 4). From this simple calculation we find fractions of NA runoff even in the Barents Sea bottom waters, which seems highly unlikely. Because we know that Ba is involved in biological processes we assume that this overestimation of f_N is caused by Ba being exported to depths below 100 m where it is released by mineralisation and we thus correct waters inside or below the LHW to $f_N = 0$. We then find NA runoff only in the central Arctic and Makarov Basin in the SML and in the Makarov Basin at depths from 50 to 100 m (fig. 6c), with fractions of up to 2%, which will be further discussed below (section 4.3). In

all other areas we find that all river runoff is from Eurasian river input $f_E = f_r$ (figs. 3-5b, 7b).

3.2 *Biological activity and freshwater in the upper water column*

In the previous distinction of NA and Eurasian river water contributions we assumed that Ba behaves conservatively. However, depletion of Ba in surface waters and export to deeper waters in the Arctic have first been shown to occur in the Chukchi Sea by Falkner et al. (1994) and Coachman and Shigaev (1992) and Ba concentrations in surface waters were as low as 12 nM. Abrahamsen et al. (2009) derived the depletion of Ba from the water mass composition, but because we have no independent way to determine the fraction of NA river water, this procedure is only applicable for those areas where this fraction can be neglected. This is largely the case in the Eurasian basins where the Pacific water fraction f_p is negligible and the presence of NA runoff therefore is very unlikely (cf. Taylor et al., 2003). In the Makarov Basin, where Pacific water is present in the surface water, we cannot a priori exclude the presence of NA runoff and we will consequently not apply calculation of Ba depletion here. For the other transects we calculate the depletion of Ba in the upper water column where we assume f_N to be zero (section 3.1):

$$Ba^0 = f_a Ba_a + f_p Ba_p + f_i Ba_i + f_E Ba_E + f_N Ba_N \quad (10)$$

$$Ba_{depl} = \frac{Ba^0 - Ba}{Ba^0} \cdot 100 \quad (11)$$

where Ba^0 is the expected Ba concentrations from the water mass fractions and the end-member concentrations (table 4). Ba_{depl} is the depletion then with positive and negative values reflecting depletion and enrichment [%], respectively (figs. 3-5c, 7c). This has to be seen as a deficit or excess concentration of Ba, based on the expected concentration Ba^0 . We find an enrichment of Ba in depths below 50 to 100 m close to the shelves (figs. 3-5c, 7c). Exceptionally large enrichment of Ba (values of Ba_{depl} as low as -61 %) is found in waters from below 20 m water depth in the Laptev Sea (fig. 7c). Depletion of Ba is found in surface waters up to 100 m in the whole area investigated (figs. 3-5c, 7c). Again we find the largest depletion in the Laptev Sea. Here we find Ba to be depleted by 31 % in the SML. A similarly large depletion of up to 28 % is found in the Barents Sea at about 80°N (fig. 3c). But depletion can also be seen in surface waters of the Amundsen Basin of section C and the Gakkel Ridge area of sections D, reaching 12 % (figs. 5c & 7c). Areas including NA runoff can be depleted as well with the underestimated American component being masked by uptake of Ba.

4 Discussion

4.1 *Balancing the fresh water fraction in the upper water column*

The equivalent water column heights (i.e. integrated fractions) of meteoric water, sea ice melt and Pacific water in the upper 50 m (fig. 8) can be compared to results from the same year and region by Abrahamsen et al. (2009). Transects of Abrahamsen et al. (2009) on the Laptev shelf towards the Eurasian Basins were farther to the east, though: 125°E from 74°N to 80°N and 130°E from 74°N to 78°N, instead of our 121°E, 75°N to 124°E, 79°N on section D (fig. 1). Cumulative river water heights in this area on our cruise range from 5 to 6 m in the Laptev Sea to about 3 m in the Eurasian Basins north of the shelf reproducing the data by Abrahamsen et al. (2009). We find large volumes of river water east of 90°E and north of 85°N (fig. 8a). In summer 2007 “onshore” atmospheric conditions prevailed in the Laptev Sea (Bauch et al., 2010). Such an “onshore” scenario forced by the prevailing wind patterns

causes Eurasian river runoff from the Laptev Sea to flow preferably eastwards into the East Siberian Sea instead of leaving the shelf northwards (Guay et al., 2001; Dmitrenko et al., 2005; Zhang et al., 2008; Bauch et al., 2009, 2011b). In the East Siberian Sea these waters may mix with local shelf waters and Pacific water from the Bering Strait. Accordingly fractions of Pacific derived waters are found at the continental slope of the East Siberian Sea in summer 2007 (Abrahamsen et al.; 2009). Based on the mass balance equations (with corrected f_N , i.e., all negative values set to zero, see section 3.1) and disregarding as first approximation biological uptake we obtained fractions of Eurasian and NA runoff (figs. 3-7b & 6c). The fraction of NA runoff in the Makarov Basin SML may be masked, however, as a result of the depletion/ uptake of Ba (Guay et al., 2009) observed in the SML of the shelves and the surface layer water of the Eurasian Basins (cf. sections 4.2, 4.3). Upon mineralization this results in an enrichment of Ba in deeper layers of water, where the fraction of NA runoff may thus be overestimated when using the five-component mass balance equations. Ba thus can be used as an indicator of biological uptake and release in areas where the abundance of NA runoff can be excluded. In areas potentially containing NA runoff, the effects of NA runoff and of biological cycling on the Ba mass balance cannot be distinguished without independent tracers. Without such additional tracers we are only able to give upper or lower limits regarding f_N . Guay et al. (2009) investigated river water components in the upper waters of the Canada Basin and detected NA runoff only in the Southern Canada Basin. Therefore it appears unlikely that the high Ba concentrations at about 100 m depth near the Alpha Ridge and Makarov Basin (fig. 6a) result from NA runoff as depicted in figure 6c. Instead, we suggest that this signal is an overestimation caused by Ba inputs from mineralisation processes in bottom waters and sediments in the Chukchi Sea. These processes have been directly observed in our dataset on the Siberian shelves (Barents and Laptev seas), but may occur also further to the east e.g. on the Chukchi Sea shelf (Falkner et al., 1994; Guay and Falkner, 1998b).

4.2 Biological activity and freshwater in the upper water column

It is important for solving eqns. 7 and 8 to assume that the meteoric fraction is composed entirely of river water and that Ba behaves conservatively (Guay et al., 2009). Alteration of water by biological activities and/ or large amounts of direct precipitation may lead to inaccuracies. While neglecting precipitation cannot cause a large error, because of the comparably large input of continental runoff to the Arctic Ocean (Aagaard and Carmack, 1989; Dickson et al., 2007) neglecting biological activity is probably causing a significant error. High biological activity is seen especially in the Barents and Laptev seas during our expedition from high carbon export shown for both regions by Cai et al. (2010) using the ^{234}Th method (2.7 and 2.9 $\text{mmol m}^{-2} \text{d}^{-1}$, respectively). In the basins where the water was covered by sea ice very low export production was observed in 2007 (0.2 $\text{mmol m}^{-2} \text{d}^{-1}$) and former years (Cai et al., 2010; Rutgers van der Loeff et al., 2002). Moreover Arrigo et al. (2008) estimate that primary production in 2007 was higher by 12.5-20.8 $\text{mol m}^{-2} \text{yr}^{-1}$ compared to 2006 in ice-free areas of the Siberian and Laptev sectors. In other ice-free areas the increase in primary production was 2.1-6.2 $\text{mol m}^{-2} \text{yr}^{-1}$ higher (Arrigo et al., 2008). Sea ice melt inventory ranges from about -2 to 1 m at the Laptev Sea continental margin in good agreement with Abrahamsen et al. (2009). Brine formation takes place mostly in the Laptev Sea and the central Arctic while in the western Eurasian Basins north of the Eurasian shelves we find net sea ice melt (fig. 8d).

Large fractions of Pacific water are found in the Makarov Basin (fig. 8c). From figs. 3-5c and 7c we see that depletion of Ba is strongest in the central Eurasian Basins and in the Laptev and Barents seas. The depletion of Ba on the shelves is consistent with the geographic pattern of ^{234}Th export and thus of the calculated carbon export flux, revealing enhanced biological activity over the Arctic shelves (Cai et al., 2010). Over the central Arctic basin, however, these authors found ^{234}Th to be near equilibrium with its parent ^{238}U and concluded extremely low carbon export in the period 1-2 months before sampling in September 2007, which would suggest that there is no reduction of Ba by biological activity here. Nonetheless we find Ba to be depleted in the upper 100-150 m of the Nansen and Amundsen Basins. This indicates that these are advected waters from the Laptev Sea or from the Barents Sea branch of the lower halocline which have been altered by biological activity and depletion of Ba in the SML and enrichment below this depth (cf. Anderson et al., 2003). We can not, however, use the depletion of PO_4 described by Anderson et al. (2003) for the years 1993-1997 to estimate the Ba depletion, because no depletion of PO_4 is seen in the Eurasian Basins in our 2007 dataset.

In the Barents Sea a 28 % depletion of Ba (fig. 3c) is accompanied by a pronounced salinity minimum in surface waters at about 80°N (cf. fig. 2a in Bauch et al., 2011a) accompanied by large net sea ice melt (fig. 8d). Just below that depth a pronounced maximum in chlorophyll concentration can be seen (cf. fig. 3 in Cai et al., 2010). This strongly suggests an origin from biological uptake at the ice edge. An elevation of Ba in deeper waters of the Barents Sea, which may have been caused by uptake of Ba into biogenic particles and release in deeper waters, is found only at station 239 with the strongest surface water depletion with 16 % enrichment (values of Ba_{depl} -16 %) at 175 m depth (fig. 3c).

The large (though not total) depletion of Ba in surface waters of the Laptev Sea is associated with low salinity similar to the correlation of the depletion of Ba with low salinity in surface waters of the Barents Sea at about 80°N (cf. fig. 3b in Bauch et al., 2011a). At the same time, though, elevated Ba concentrations are encountered in deeper waters of the Laptev Sea. While the depletion in surface waters is about 26 to 31 % of the expected concentration, Ba in shelf water of the Laptev Sea is elevated by up to 61 % close to the bottom (fig. 7c). The gradient with depletion in the SML and enrichment in the underlying waters is exceptionally large. Abrahamsen et al. (2009) suggested biological export to be responsible, which is reasonable due to the patterns of ^{234}Th in the Laptev Sea (Cai et al., 2010). Moreover Anderson et al. (2009) have shown that in the Laptev Sea organic matter is dominantly of terrestrial origin and to a smaller degree of marine origin. In the Laptev Sea this terrigenous organic matter may thus have an important role in redistributing the elements by scavenging and/ or remineralization at depth, while autochthonous production is more important in the East Siberian Sea (Anderson, pers. comm.).

4.3 Intrusions of Chukchi Sea water in the upper halocline

In 100 m depth at station 342 positioned on the southern Alpha Ridge and neighboring stations 338 and 349 we find pronounced maxima of Ba (fig. 6a) and silicate (cf. fig. 11a in Middag et al., 2009) together with other nutrients (not shown). These maxima are found at the lower end of a maximum of the Pacific water fraction at 50 to 75 m water depth and these waters are identified by a salinity of 32.5 to 33.3 and their nutrient concentrations to be part of the UHW. At the lower end of the UHW at 120 m depth a pronounced minimum is seen in oxygen (fig. 9). Both could be

explained by a layer of winter water from the bottom of the Chukchi Sea (cf. Woodgate et al., 2005) reaching into the Makarov Basin. These waters are enhanced in nutrients and reduced in oxygen by bacterial consumption of the summer bloom (Cooper et al., 1999; Walsh et al., 1989). While nutrients are released into the water column over the Chukchi shelf oxygen consumption is largest close to the bottom. Unfortunately there is no Ba data available at the depth of the oxygen minimum (120 m) but we expect high concentrations of Ba, because in addition to release from biological particles Ba has also a source in sediments. Looking at the Ba and silicate (Middag et al., 2009) we see that this water with low oxygen and high Ba at the lower end of the UHW reaches far north into the Makarov Basin. In this water mass we calculate large fractions of NA runoff. As mentioned above (cf. 4.1) it is unlikely that this truly is NA runoff but rather water from the winter layer of the Chukchi Sea. Regardless of the Ba source we are able to identify water from the Chukchi shelf by support of other data (e.g. high silicate concentrations and high AOU) in depths of 50 to 100 m in the southern Makarov Basin and over the Alpha and Mendeleev Ridges.

Conclusions

Dissolved Ba has to be used carefully as a tracer of river water sources because of its non-conservative behavior (Abrahamsen et al., 2009; Guay et al., 2009). Strong removal of 25 to 31 % is observed over the Barents and Laptev shelves. On the Eurasian shelves terrestrial components have an important role in the vertical distribution of dissolved Ba.

In the central Eurasian Basins we find surface waters depleted in Ba and close to the shelves Ba-enriched water below 100 m. ^{234}Th data show very low organic export in the basins in the 1-2 months preceding our sampling. The Ba depletion and enrichment may have been caused by biological activity older than the 1-2 months covered by the ^{234}Th method, which means that it may well have been advected from the shelves. This implies that even in the central Arctic we would need additional parameters such as ^{234}Th , nutrients, or oxygen to correct for these processes before we can use Ba to distinguish between American and Eurasian river waters. If in a seasonally less ice-covered or even ice-free Arctic Ocean primary production would increase the use of Ba as tracer for river sources would be even more questionable.

In the Makarov Basin enhanced Ba concentrations can be ascribed to Pacific water reaching as far as the Lomonosov Ridge, except for the southernmost stations at depths of about 50-100 m. We suggest that the alleged NA runoff in this area is a diagenetic signal originating in the Chukchi Sea winter layer instead. In agreement with Guay et al. (2009) Ba signals cannot unequivocally show the presence of NA river water anywhere in the area of our cruise.

Nonetheless export of Ba to bottom waters on the shelves allows us to track these waters in the central Arctic basins and the depletion of Ba in upper waters brings evidence of export by biological production. We finally assume that Ba as a tracer of river water stays important in areas covered by sea ice and thus low productivity.

Acknowledgements

This work has been funded by the EU Sixth Framework Programme DAMOCLES (Developing Arctic Modelling and Observing Capabilities for Long-term Environment Studies), contract number 018509GOCE.

Also the good support by people from the IPY (International Polar Year) and the GEOTRACES program (international study of the global marine biogeochemical cycles of trace elements and their isotopes) has to be emphasized.

Special thanks go to Sabine Mertineit who helped in acquiring the Ba samples during Polarstern cruise ARK-XXII/2. We thank K. Bakker from nutrient department of Royal Netherlands Institute for Sea Research (NIOZ) for data on silicate and nutrients. Moreover we have to thank Prof. Hein De Baar from the NIOZ who made possible the access to their archived samples as well as Rob Middag and Maarten Klunder from the NIOZ for their cooperative help. We further thank A. Wisotzki from AWI oceanography group for supporting the oxygen data. D. Bauch was financially supported by the DFG under grant SP526/3.

We thank Catherine Jeandel, Erika Sternberg, Frank Dehairs, Kristin Orians and Yiming Luo for their participation in the interlab comparison and Kelly Falkner for helpful discussions on the calibration issue.

References

- Aagaard, K. and Carmack, E.C., 1989. The Role of Sea Ice and Other Fresh-Water in the Arctic Circulation. *Journal of Geophysical Research C: Oceans*, 94(C10): 14485-14498, doi:10.1029/JC094iC10p14485.
- Aagaard, K., Coachman, L.K., Carmack, E., 1981. On the Halocline of the Arctic Ocean. *Deep-Sea Research Part I: Oceanographic Research Papers*, 28(6): 529-545, doi:10.1016/0198-0149(81)90115-1.
- Abrahamsen, E.P., Meredith, M.P., Falkner, K.K., Torres-Valdes, S., Leng, M.J., Alkire, M.B., Bacon, S., Laxon, S.W., Polyakov, I., Ivanov, V., 2009. Tracer-derived freshwater composition of the Siberian continental shelf and slope following the extreme Arctic summer of 2007. *Geophysical Research Letters*, 36: 5 pp., doi:10.1029/2009gl037341.
- Anderson, L. G., Jones, E. P., and Swift, J. H., 2003. Export production in the central Arctic Ocean evaluated from phosphate deficits. *Journal of Geophysical Research C: Oceans*, 108(3199): 6 pp., doi:10.1029/2001JC001057.
- Anderson, L.G., Jutterström, S., Hjalmarsson, S., Wählström, I., Semiletov, I.P., 2009. Out-gassing of CO₂ from Siberian Shelf seas by terrestrial organic matter decomposition. *Geophysical Research Letters*, 36(L20601): 6 pp., doi:10.1029/2009GL040046.
- Arrigo, K.R., van Dijken, G., Pabi, S., 2008. Impact of a shrinking Arctic ice cover on marine primary production. *Geophysical Research Letters*, 35(L19603): 6 pp., doi:10.1029/2008GL035028.
- Bauch, D., R. v. d. Loeff, M., Andersen, N., Torres-Valdes, S., Bakker, K. and Abrahamsen, E.P., 2011a. Origin of freshwater and polynya water in the Arctic Ocean halocline in summer 2007. *Progress in Oceanography*, doi:10.1016/j.pocean.2011.07.017.
- Bauch, D., Gröger, M., Dmitrenko, I., Hölemann, J., Kirillov, S., Mackensen, A., Taldenkova, E., Andersen, N., 2011b. Atmospheric controlled freshwater release at the Laptev Sea Continental margin, *Polar Research*, 30: 5858-5871, doi:10.3402/polar.v30i0.5858.
- Bauch, D., Hölemann, J., Willmes, S., Gröger, M., Novikhin, A., Nikulina, A., Kassens, H., Timokhov, L., 2010. Changes in distribution of brine waters on the Laptev Sea shelf in 2007. *Journal of Geophysical Research*, 115(C11008): 11 pp., doi:10.1029/2010JC006249.

- Bauch, D., Dmitrenko, I.A., Wegner, C., Hölemann, J.A., Kirillov, S.A., Timokhov, L.A., Kassens, H., 2009. Exchange of Laptev Sea and Arctic Ocean halocline waters in response to atmospheric forcing. *Journal of Geophysical Research C: Oceans*, 114(C05008): 8 pp., doi:10.1029/2008JC005062.
- Bauch, D., Schlosser, P., Fairbanks, R.G., 1995. Freshwater balance and the sources of deep and bottom waters in the Arctic Ocean inferred from the distribution of H₂¹⁸O. *Progress in Oceanography*, 35(1): 53-80, doi:10.1016/0079-6611(95)00005-2.
- Bernstein, R.E., Byrne, R.H., Betzer, P.R., Greco, A.M., 1992. Morphologies and transformations of celestite in seawater: The role of acantharians in strontium and barium geochemistry. *Geochimica et Cosmochimica Acta*, 56(8): 3273-3279, doi:10.1016/0016-7037(92)90304-2.
- Bernstein, R.E., Byrne, R.H., Schijf, J., 1998. Acantharians: a missing link in the oceanic biogeochemistry of barium. *Deep Sea Research Part I: Oceanographic Research Papers*, 45(2-3): 491-505, doi:10.1016/S0967-0637(97)00095-2.
- Bishop, J.K.B., 1988. The barite-opal-organic carbon association in oceanic particulate matter. *Nature*, 332(6162): 341-343, doi:10.1038/332341a0.
- Björk, G. and Söderkvist, J., 2002. Dependence of the Arctic Ocean ice thickness distribution on the poleward energy flux in the atmosphere. *Journal of Geophysical Research C: Oceans*, 107(3173): 17 pp., doi:10.1029/2000jc000723.
- Broecker, W.S., Takahashi, T., Takahashi, T., 1985. Sources and flow patterns of deep-ocean waters as deduced from potential temperature, salinity, and initial phosphate concentration. *Journal of Geophysical Research*, 90(C10): 6925-6939, doi:10.1029/JC090iC04p06925.
- Cai, P., Rutgers van der Loeff, M., Stimac, I., Nöthig, E.-M., Lepore, K., Moran, S.B., 2010. Low export flux of particulate organic carbon in the central Arctic Ocean as revealed by ²³⁴Th:²³⁸U disequilibrium. *Journal of Geophysical Research C: Oceans*, doi:10.1029/2009JC005595.
- Carroll, J., Falkner, K.K., Brown, E.T., Moore, W.S., 1993. The role of the Ganges-Brahmaputra mixing zone in supplying barium and ²²⁶Ra to the Bay of Bengal. *Geochimica et Cosmochimica Acta*, 57(13): 2981-2990, doi:10.1016/0016-7037(93)90287-7.
- Chan, L.H., Drummond, D., Edmond, J.M., Grant, B., 1977. On the barium data from the Atlantic GEOSECS expedition. *Deep Sea Research*, 24(7): 613-649, doi:10.1016/0146-6291(77)90505-7.
- Coachman, L.K., Shigaev, V.V., 1992. Northern Bering-Chukchi Sea Ecosystem: The Physical Basis. In: P.A. Nagel (Editor), *Results of the third joint US-USSR Bering & Chukchi Seas expedition (BERPAC): Summer 1988*. U.S. Fish and Wildlife Service, Washington, DC : pp. 17-27.
- Collier, R., Edmond, J., 1984. The trace element geochemistry of marine biogenic particulate matter. *Progress In Oceanography*, 13(2): 113-199, doi:10.1016/0079-6611(84)90008-9.
- Comiso, J.C., Parkinson, C.L., Gersten, R., Stock, L., 2008. Accelerated decline in Arctic sea ice cover. *Geophysical Research Letters*, 35(L01703): 6 pp., doi:10.1029/2007GL031972.
- Cooper, L.W., Cota, G.F., Pomeroy, L.R., Grebmeier, J.M., Whitley, T.E., 1999. Modification of NO, PO, and NO/PO during flow across the Bering and Chukchi shelves: Implications for use as Arctic water mass tracers. *Journal of*

- Geophysical Research C: Oceans, 104(C4): 7827-7836, doi:10.1029/1999JC900010.
- Cooper, L.W., McClelland, J.W., Holmes, R.M., Raymond, P.A., Gibson, J.J., Guay, C.K., Peterson, B.J., 2008. Flow-weighted values of runoff tracers ($\delta^{18}\text{O}$, DOC, Ba, alkalinity) from the six largest Arctic rivers. *Geophysical Research Letters*, 35(L18606): 5 pp., doi:10.1029/2008gl035007.
- Craig, H., 1961. Standard for Reporting Concentrations of Deuterium and Oxygen-18 in Natural Waters. *Science*, 133(3467): 1833-1834, doi:10.1126/science.133.3467.1833.
- De Baar, H.J.W., Timmermans, K.R., Laan, P., De Porto, H.H., Ober, S., Blom, J.J., Bakker, M.C., Schilling, J., Sarthou, G., Smit, M.G., Klunder, M., 2008. Titan: A new facility for ultraclean sampling of trace elements and isotopes in the deep oceans in the international Geotraces program. *Marine Chemistry*, 111(1-2): 4-21, doi:10.1016/j.marchem.2007.07.009.
- Dehairs, F., Chesselet, R., Jedwab, J., 1980. Discrete suspended particles of barite and the barium cycle in the open ocean. *Earth and Planetary Science Letters*, 49(2): 528-550, doi:10.1016/0012-821X(80)90094-1.
- Dickson, R., Rudels, B., Dye, S., Karcher, M., Meincke, J., Yashayaev, I., 2007. Current estimates of freshwater flux through Arctic and subarctic seas. *Progress in Oceanography*, 73(3-4): 210-230, doi:10.1016/j.pocean.2006.12.003.
- Dmitrenko, I., Kirillov, S., Eicken, H., Markova, N., 2005. Wind-driven summer surface hydrography of the eastern Siberian shelf. *Geophysical Research Letters*, 32(L14613): 5 pp., doi:10.1029/2005GL023022.
- Dymond, J., Suess, E., Lyle, M., 1992. Barium in Deep-Sea Sediment: A Geochemical Proxy for Paleoproductivity. *Paleoceanography*, 7(2): 163-181, doi:10.1029/92PA00181.
- Edmond, J.M., Measures, C., McDuff, R.E., Chan, L.H., Collier, R., Grant, B., Gordon, L.I., Corliss, J. B., 1979. Ridge crest hydrothermal activity and the balances of the major and minor elements in the ocean: The Galapagos data. *Earth and Planetary Science Letters*, 46(1): 1-18, doi:10.1016/0012-821X(79)90061-X.
- Ekwurzel, B., Schlosser, P., Mortlock, R.A., Fairbanks, R.G., Swift, J.H., 2001. River runoff, sea ice meltwater, and Pacific water distribution and mean residence times in the Arctic Ocean. *Journal of Geophysical Research C: Oceans*, 106(C5): 9075-9092.
- Esser, B.K. and Volpe, A.M., 2002. At-sea high-resolution chemical mapping: extreme barium depletion in North Pacific surface water. *Marine Chemistry*, 79(2): 67-79, doi:10.1016/S0304-4203(02)00037-3.
- Falkner, K.K., Klinkhammer, G.P., Bowers, T.S., Todd, J.F., Lewis, B.L., Landing, W.M., Edmond, J.M., 1993. The behavior of barium in anoxic marine waters. *Geochimica et Cosmochimica Acta*, 57(3): 537-554, doi:10.1016/0016-7037(93)90366-5.
- Falkner, K.K., MacDonald, R.W., Carmack, E.C., Weingartner, T., 1994. The potential of barium as a tracer of Arctic water masses. In: O.M. Johannessen, R.D. Muench and J.E. Overland (Editors), *The Polar Oceans and Their Role in Shaping the Global Environment: The Nansen Centennial Volume*, AGU Geophysics Monograph Series. American Geophysical Union, Washington, DC, pp. 63-76.
- Freydier, R., Dupré, B., Polve, M., 1995. Analyses by Inductively-Coupled Plasma-Mass Spectrometry of Ba Concentrations in Water and Rock Samples -

- Comparison between Isotope-Dilution and External Calibration with or without Internal Standard. *European Mass Spectrometry*, 1(3): 283-291.
- Guay, C.K. and Falkner, K.K., 1998a. A survey of dissolved barium in the estuaries of major Arctic rivers and adjacent seas. *Continental Shelf Research*, 18(8): 859-882, doi:10.1016/S0278-4343(98)00023-5.
- Guay, C.K. and Falkner, K.K., 1998b. Barium as a tracer of Arctic halocline and river waters. *Deep-Sea Research Part II: Topical Studies in Oceanography*, 44(8): 1543-1569, doi:10.1016/S0967-0645(97)00066-0.
- Guay, C.K.H., Falkner, K.K., Muench, R.D., Mensch, M., Frank, M., Bayer, R., 2001. Wind-driven transport pathways for Eurasian Arctic river discharge. *Journal of Geophysical Research C: Oceans*, 106(C6): 11469-11480, doi:10.1029/2000JC000261.
- Guay, C.K.H., McLaughlin, F.A., Yamamoto-Kawai, M., 2009. Differentiating fluvial components of upper Canada Basin waters on the basis of measurements of dissolved barium combined with other physical and chemical tracers. *Journal of Geophysical Research C: Oceans*, 114(C00A09): 17 pp., doi:10.1029/2008JC005099.
- Hanor, J.S. and Chan, L.-H., 1977. Non-conservative behavior of barium during mixing of Mississippi River and Gulf of Mexico waters. *Earth and Planetary Science Letters*, 37(2): 242-250, doi:10.1016/0012-821X(77)90169-8.
- Jones, E.P. and Anderson, L.G., 1986. On the Origin of the Chemical Properties of the Arctic Ocean Halocline. *Journal of Geophysical Research C: Oceans*, 91(C9): 10759-10767, doi:10.1029/JC091iC09p10759.
- Jones, E., Anderson, L., and Swift, J., 1998. Distribution of Atlantic and Pacific water in the upper Arctic Ocean: Implications for circulation. *Geophysical Research Letters*, 25(6), 765-768.
- Jones, E.P., Anderson, L.G., Jutterström, S., Mintrop, L., and Swift, J.H., 2008. Pacific freshwater, river water and sea ice meltwater across Arctic Ocean basins: Results from the 2005 Beringia Expedition. *Journal of Geophysical Research*, 113(C08012): 10 pp., doi:10.1029/2007JC004124.
- Klinkhammer, G.P. and Chan, L.H., 1990. Determination of barium in marine waters by isotope dilution inductively coupled plasma mass spectrometry. *Analytica Chimica Acta*, 232: 323-329, doi:10.1016/S0003-2670(00)81249-0.
- Lea, D.W. and Boyle, E.A., 1990. Foraminiferal Reconstruction of Barium Distributions in Water Masses of the Glacial Oceans. *Paleoceanography*, 5(5): 719-742, doi:10.1029/PA005i005p00719.
- Li, Y.-H. and Chan, L.-H., 1979. Desorption of Ba and ²²⁶Ra from river-borne sediments in the Hudson estuary. *Earth and Planetary Science Letters*, 43(3): 343-350, doi:10.1016/0012-821X(79)90089-X.
- Martin, J.-M. and Meybeck, M., 1979. Elemental mass-balance of material carried by major world rivers. *Marine Chemistry*, 7(3): 173-206, doi:10.1016/0304-4203(79)90039-2.
- Middag, R., de Baar, H.J.W., Laan, P., Bakker, K., 2009. Dissolved aluminium and the silicon cycle in the Arctic Ocean. *Marine Chemistry*, 115(3-4): 176-195, doi:10.1016/j.marchem.2009.08.002.
- Morison, J., Steele, M., Andersen, R., 1998. Hydrography of the upper Arctic Ocean measured from the nuclear submarine USS Pargo. *Deep-Sea Research Part I: Oceanographic Research Papers*, 45(1): 15-38, doi:10.1016/S0967-0637(97)00025-3.

- Östlund, H.G. and Hut, G., 1984. Arctic Ocean Water Mass Balance from Isotope Data. *Journal of Geophysical Research C: Oceans*, 89(NC4): 6373-6381, doi:10.1029/JC089iC04p06373.
- Rabe, B., Schauer, U., Mackensen, A., Karcher, M., Hansen, E., Beszczynska-Möller, A., 2009. Freshwater components and transports in the Fram Strait - recent observations and changes since the late 1990s. *Ocean Science*, 5(3): 219-233, doi:10.5194/osd-6-581-2009.
- Rabe, B., Karcher, M., Schauer, U., Toole, J. M., Krishfield, R. A., Pisarev, S., Kauker, F., Gerdes, R., Kikuchi, T., 2011. An assessment of Arctic Ocean freshwater content changes from the 1990s to the 2006-2008 period. *Deep Sea Research Part I: Oceanographic Research Papers* 58: 173-185 doi:10.1016/j.dsr.2010.12.002.
- Roeske, T., Rutgers van der Loeff, M.M., Bauch, D., 2011. Barium measured on water bottle samples during POLARSTERN cruise ARK-XXII/2 (SPACE). <http://doi.pangaea.de/10.1594/PANGAEA.758745>.
- Roeske, T., Middag, R., Bakker, K., Rutgers van der Loeff, M. M., submitted to *Marine Chemistry*. Deep water circulation and shelf water inputs to the Arctic Ocean by dissolved Ba.
- Rudels, B., Jones, E.P., Schauer, U., Eriksson, P., 2004. Atlantic sources of the Arctic Ocean surface and halocline waters. *Polar Research*, 23(2): 181-208, Doi:10.1111/j.1751-8369.2004.tb00007.x.
- Rutgers van der Loeff, M.M., Meyer, R., Rudels, B., Rachor, E., 2002. Resuspension and particle transport in the Benthic Nepheloid Layer in and near Fram Strait in relation to faunal abundances and ²³⁴Th depletion. *Deep-sea Research*, 49(11): 1941–1958, doi:10.1016/S0967-0637(02)00113-9.
- Schauer, U., 2008. The expedition ARKTIS-XXII/2 of the research vessel "Polarstern" in 2007. *Berichte zur Polar- und Meeresforschung = Reports on polar and marine research*(579): 271 pp.
- Schlitzer, R., 2010. Ocean Data View, <http://odv.awi.de>, latest access on March 30, 2011.
- Serreze, M.C., Barrett, A.P., Slater, A.G., Woodgate, R.A., Aagaard, K., Lammers, R.B., Steele, M., Moritz, R., Meredith, M., Lee, C. M., 2006. The large-scale freshwater cycle of the Arctic. *Journal of Geophysical Research C: Oceans*, 111(C11010): 19 pp., doi:10.1029/2005JC003424.
- Shimada, K., Itoh, M., Nishino, S., McLaughlin, F., Carmack, E., Proshutinsky, A., 2005. Halocline structure in the Canada Basin of the Arctic Ocean. *Geophysical Research Letters*, 32(L03605): 5 pp., doi:10.1029/2004GL021358.
- Taylor, J.R., Falkner, K.K., Schauer, U., Meredith, M., 2003. Quantitative considerations of dissolved barium as a tracer in the Arctic Ocean. *Journal of Geophysical Research C: Oceans*, 108(12): 4-1, doi:10.1029/2002JC001635.
- Von Damm, K.L., 1990. Seafloor Hydrothermal Activity: Black Smoker Chemistry and Chimneys. *Annual Review of Earth and Planetary Sciences*, 18(1): 173-204, doi:10.1146/annurev.ea.18.050190.001133.
- Von Damm, K.L., Edmond, J.M., Grant, B., Measures, C.I., Walden, B., Weiss, R.F., 1985. Chemistry of submarine hydrothermal solutions at 21°N, East Pacific Rise. *Geochimica et Cosmochimica Acta*, 49(11): 2197-2220, doi:10.1016/0016-7037(85)90222-4.
- Walsh, J.J., McRoy, C.P., Coachman, L.K., Goering, J.J., Nihoul, J.J., Whitley, T.E., Blackburn, T.H., Parker, P.L., Wirrick, C.D., Shuert, P. G., 1989. Carbon and nitrogen cycling within the Bering/Chukchi Seas: Source regions for

- organic matter effecting AOU demands of the Arctic Ocean. *Progress In Oceanography*, 22(4): 277-359, doi:10.1016/0079-6611(89)90006-2.
- Weingartner, T.J., Cavalieri, D.J., Aagaard, K., Sasaki, Y., 1998. Circulation, dense water formation, and outflow on the northeast Chukchi shelf. *Journal of Geophysical Research C: Oceans*, 103(C4): 7647-7661.
- Wisotzki, A (2008): Physical oceanography measured on water bottle samples during POLARSTERN cruise ARK-XXII/2. Alfred Wegener Institute for Polar and Marine Research, Bremerhaven, doi:10.1594/PANGAEA.759285.
- Woodgate, R.A., Aagaard, K., Swift, J.H., Falkner, K.K., Smethie, W.M., Jr., 2005. Pacific ventilation of the Arctic Ocean's lower halocline by upwelling and diapycnal mixing over the continental margin. *Geophysical Research Letters*, 32(L18609): 5 pp., doi:10.1029/2005GL023999.
- Yamamoto-Kawai, M., McLaughlin, F.A., Carmack, E.C., Nishino, S., Shimada, K., 2008. Freshwater budget of the Canada Basin, Arctic Ocean, from salinity, $\delta^{18}\text{O}$, and nutrients. *Journal of Geophysical Research C: Oceans*, 113(C1): 12, doi:10.1029/2006JC003858.
- Zhang, J.L., Lindsay, R., Steele, M., Schweiger, A., 2008. What drove the dramatic retreat of arctic sea ice during summer 2007? *Geophysical Research Letters*, 35(L11505): 5 pp., doi:10.1029/2008gl034005.

Table 1: Station positions with Ba data available on ARK-XXII/2 in degrees latitude and longitude (first position of the station log).

Section	Station	Lat. °N	Lon. °E	Section	Station	Lat. °N	Lon. °E
A	228	75°0.03'	33°59.95'	C1	306	85°55.37'	91°7.26'
	236	77°30.04'	33°59.79'		309	87°2.74'	104°47.21'
	237	78°59.83'	33°59.68'		310	87°39.46'	112°2.23'
	239	80°59.69'	33°59.76'	C2	316	88°10.58'	139°37.07'
	246	81°52.10'	34°0.72'		319	88°39.86'	153°39.66'
	255	82°30.20'	33°57.12'		326	88°1.71'	170°5.23'
	258	83°59.93'	34°0.62'		328	87°49.80'	-170°34.10'
	260	84°29.36'	36°8.31'		333	87°1.68'	-146°23.98'
B	261	84°38.72'	60°56.02'		338	85°42.25'	-135°2.35'
	266	83°8.27'	61°44.46'		342	84°30.00'	-138°25.12'
	271	82°30.18'	60°47.71'	349	85°3.83'	-164°28.14'	
	272	82°15.12'	61°59.76'	D	371	84°39.19'	102°44.18'
	276	82°5.05'	68°57.50'		373	84°11.93'	108°56.10'
C1	279	81°14.71'	86°12.13'		379	82°51.93'	117°49.73'
	285	82°8.51'	86°19.75'		382	81°21.45'	120°43.12'
	291	82°42.61'	86°15.92'		385	79°21.14'	124°21.63'
	295	83°16.33'	86°16.97'	389	78°21.30'	124°30.89'	
	299	84°3.06'	89°2.53'	400	77°23.29'	123°24.02'	
	301	84°34.81'	89°50.14'	407	76°10.83'	122°7.72'	
	302	84°53.56'	90°3.27'	411	75°12.00'	121°21.45'	

Table 2: Dissolved Ba concentrations and methodical errors (Roeske et al., 2011), temperature, salinity, dissolved oxygen (courtesy of AWI oceanography group, Schauer et al., 2008) and phosphate (courtesy of nutrient department of Royal Netherlands Institute for Sea Research, Karel Bakker pers. comm.):

Station	depth [m]	Ba [nM]	error [nM]	T [°C]	Salinity	O ₂ [μM]	PO ₄ [μM]	Station	depth [m]	Ba [nM]	error [nM]	T [°C]	Salinity	O ₂ [μM]	PO ₄ [μM]
228	25.5	42.5	0.7	4.0787	35.0541	337.2	0.185	306	50.3	45	0.7	-1.8023	33.7654	335.2	0.427
	49.4	42.8	0.8	2.7962	35.0909	323.5	0.672		100.6	42.2	1.3	-1.2953	34.2115	293.1	0.662
	74.7	42.9	0.5	2.1408	35.0862	327.0	0.608		150.6	41.7	1.2	0.0499	34.5286	284.6	0.751
	100	43.6	0.8	1.1902	35.049	326.8	0.671		200.6	42.1	0.8	1.0434	34.7767	279.1	0.82
236	4.7	40.1	0.7	2.6546	33.9547	327.8	0.051	309	5.1	48.6	0.9	-1.6876	31.7575	366.6	0.223
	24.8	41.8	0.8	-0.1154	34.2691	385.8	0.144		25.2	51.3	0.7	-1.6847	32.6497	351.6	0.355
	50.6	44.2	0.8	-1.57	34.5182	327.7	0.612		50.2	49.5	0.8	-1.7606	33.133	335.8	0.449
	74.9	42.9	0.7	-1.4798	34.5731	316.9	0.659		75.3	44.7	0.8	-1.6313	33.873	301.5	0.615
	100.3	44.7	0.8	0.3147	34.7322	293.7	0.794		100.6	43.9	1.2	-1.2821	34.2176	295.3	0.651
	125.6	43.4	0.8	1.1487	34.8809	301.9	9999		148.4	42.3	1.2	-0.0164	34.5275	288.6	0.727
	150.5	43.9	0.7	1.6797	34.976	309.6	0.827		200.6	44.7	0.7	1.041	34.7915	282.1	0.806
237	24.9	41.3	0.8	-1.5191	34.2311	340.8	0.453	310	8.9	57.8	0.9	-1.6688	31.6038	371.7	0.187
	50	41.6	0.9	-1.5516	34.3294	319.0	0.557		25	48.3	0.8	-1.6529	31.9104	364.8	0.249
	75.5	42.7	0.8	-1.2634	34.453	315.1	0.615		49.8	48.8	0.7	-1.7348	32.7625	336.6	0.451
	99.8	42.6	0.7	-0.7816	34.537	310.5	0.655		100	43.9	0.8	-1.3112	34.2115	294.3	0.656
	124.8	42.3	0.7	0.2784	34.6578	298.1	0.721		150.1	41.9	1.2	-0.0472	34.5106	287.9	0.72
	150.3	43.5	0.8	0.7953	34.7228	291.0	0.766		200.3	41.6	1.2	0.8723	34.7675	279.9	0.811
	174.4	44.3	0.7	1.027	34.7663	286.8	0.804		316	4.7	48.6	0.8	-1.6764	31.1637	372.3
	200	44.7	0.8	1.5849	34.8604	279.8	0.861	24.9		51.6	1.3	-1.6422	31.8107	350.7	0.402
239	225.6	44.2	1.1	1.4828	34.894	302.0	0.894	49.9	51.3	1.2	-1.7168	32.5013	327.2	0.559	
	4.6	30.3	0.8	-0.9704	32.6638	388.4	0.044	54	49.3	1.4	-1.7102	32.6526	319.2	0.612	
	24.7	31	0.7	-0.872	33.9182	370.1	0.148	75.2	46.2	1.2	-1.6032	33.8435	295.8	0.65	
	50.1	40.4	0.7	-0.7108	34.3545	324.0	0.549	100.2	44.5	1.4	-1.3198	34.1767	292.8	0.691	
	75.2	43.4	0.8	-0.2388	34.4803	309.8	0.679	319	5	53.1	0.8	-1.6356	30.424	375.5	0.293
	100.3	44	0.7	0.5419	34.6237	297.8	0.765		21.9	54.1	1	-1.6281	30.5639	369.9	0.425
	125	42.9	0.7	0.8113	34.6611	296.5	0.776		50	54.8	1.3	-1.7309	32.4774	327.9	0.604
	148.2	43.3	0.7	0.8321	34.6674	297.3	0.784		100.1	45.5	1.2	-1.3708	34.116	289.0	0.689
175.2	50.3	0.7	0.8862	34.719	298.5	0.797	200.8		43.4	1.2	0.5105	34.6732	276.0	0.823	
246	4.4	39.3	0.7	-1.3879	32.936	391.3	0.112	326	9.6	59.9	0.8	-1.5531	29.2911	365.3	0.459
	24.7	41.9	0.8	-1.5982	34.0838	327.0	0.587		24.1	60.9	0.8	-1.5328	30.3682	361.0	0.505
	50.2	42.4	0.9	-1.3636	34.3529	314.6	0.696		75.3	48.4	1.3	-1.6047	33.4606	283.1	0.782

	100.2	42.3	0.7	2.0208	34.8279	288.0	0.796		100.3	43.8	1.7	-1.497	34.0318	283.6	0.702
	200.7	42.3	0.9	2.7628	34.9903	285.6	0.824		149.9	46.1	0.7	-0.5068	34.4092	283.2	0.735
	249.4	42.6	0.8	2.5975	34.9911	285.7	0.835		200.1	49.5	1.2	0.3494	34.6481	275.3	0.814
255	18.6	42.2	1.1	-1.6693	34.0832	307.8	0.563	328	5	64.5	1	-1.5387	28.9468	386.0	0.4
	37.4	43	0.9	-1.7694	34.2651	298.2	0.642		24.6	61.4	2.7	-1.5311	30.2788	378.9	0.448
	98.1	43.1	0.7	1.9553	34.7919	276.0	0.795		50	58.9	1.5	-1.6435	31.1305	368.0	0.595
	199.5	42.6	1.4	2.6914	34.9578	275.6	0.823		75.6	50.5	5.8	-1.6049	33.1995	299.5	0.96
258	4.5	41.8	0.8	-1.6802	33.7842	343.0	0.399		100.5	45.2	1.7	-1.5229	33.9607	303.1	0.714
	17.5	41.7	0.9	-1.6993	34.0365	339.8	0.421		150.3	43.2	0.8	-0.5355	34.3968	300.2	0.748
	40	42.1	0.8	-1.8	34.1832	330.1	0.497		200.6	44.3	1.3	0.301	34.6273	291.9	0.82
	99.5	42.4	0.9	-1.2023	34.3346	304.5	0.593	333	7.8	60.3	0.7	-1.5496	28.7277	373.4	0.532
	200	45	1.2	2.0406	34.8827	275.7	0.853		23.9	61.6	1	-1.5379	28.8438	371.5	0.593
260	4.7	42.5	0.7	-1.6723	33.8614	364.0	0.37		49.4	59.8	1.2	-1.5671	30.1146	351.6	0.921
	24.4	42.3	0.8	-1.7041	34.0272	364.1	0.374		99.8	44.3	1.3	-1.5395	33.9081	283.3	0.732
	49.5	41	0.9	-1.8189	34.1835	363.9	0.382		149.8	43.1	0.7	-0.7976	34.3575	285.6	0.722
	74.3	42.2	0.9	-1.8317	34.2029	354.7	0.442		199.6	41.6	1.1	0.0491	34.5865	281.3	0.782
	99.9	44.2	0.8	-1.7668	34.2298	351.0	0.551	338	5.3	62.1	0.8	-1.535	28.585	373.0	0.807
	149.7	42.1	1.3	1.2987	34.6852	343.6	0.521		24.6	61.9	1.3	-1.39	29.7106	375.9	0.858
	200.1	42.7	1.2	2.0338	34.864	293.7	0.832		50.3	59.4	1.5	-1.5856	30.2997	370.1	0.942
261	4.1	42.2	0.8	-1.5897	33.382	362.2	0.289		75.2	61.9	1.2	-1.5316	31.9056	292.2	1.576
	25.4	42.9	0.8	-1.697	33.9838	341.4	0.43		100.7	53.1	0.9	-1.4984	33.2897	263.0	1.102
	50.2	42.2	0.8	-1.8221	34.1618	328.9	0.509		150.3	43.6	0.8	-0.946	34.2266	282.3	0.769
	75.6	42.8	0.8	-1.8357	34.1843	325.8	0.53		200	42.4	1.2	-0.1259	34.5176	270.5	0.872
	100.6	41.8	1.3	-1.1429	34.279	307.2	0.667	342	10	58	0.9	-1.4696	29.2901	377.7	0.824
	201.2	42.3	0.7	2.2379	34.875	278.8	0.806		25.2	59	1.2	-1.4349	30.2968	381.8	0.841
266a	3.8	40.6	0.8	-1.641	33.3143	300.4	0.256		50.5	59.1	1.3	-1.5895	30.51	376.8	0.884
	23.2	41.2	0.9	-1.4261	33.7782	313.5	0.389		75.5	61.2	1.2	-1.5047	31.4757	318.6	1.559
	50.1	43.5	1	1.3357	34.7015	279.0	0.741		100.8	68	0.8	-1.3774	32.5126	244.8	1.94
	100.2	43.8	0.7	2.6667	34.9003	274.4	0.786		150.6	45.1	1	-1.1954	34.0809	281.4	0.78
	199.8	45	1.3	2.6487	34.9565	276.5	0.807		200.3	43.1	1.3	-0.4155	34.4127	273.3	0.833
266b	5	40.7	0.7	-1.63	33.0568	378.4	0.179	349	9.2	66.4	0.8	-1.3983	26.9659	383.0	0.705
	24.8	42.6	0.8	-1.2084	34.1101	336.3	0.573		24.9	66.5	1.2	-1.4828	29.0032	386.8	0.723
	49.8	44.3	0.7	1.1544	34.6408	307.9	0.733		50.2	59.8	1.5	-1.5414	31.1274	339.1	1.1
	99.9	43.7	0.8	2.5363	34.8827	294.8	0.778		75.1	55.2	1.3	-1.5513	32.8902	291.3	1.096
	199.9	44	1.4	2.7059	34.9623	298.3	0.802		100.7	46.1	0.9	-1.5422	33.869	298.0	0.775
271	5	40.6	0.8	-1.5182	32.8458	362.8	0.161		150.3	44.1	0.8	-0.6942	34.3371	297.5	0.76

272	4.8	40.6	0.9	-1.6348	32.6607	365.4	0.173		200.6	42.7	1.3	0.1651	34.5988	291.9	0.817	
276	5	42.3	0.8	-1.692	32.9036	370.1	0.191	371	9.5	47.2	0.7	-1.689	33.1565	356.1	0.307	
	25.1	42.8	0.8	-1.5777	33.814	342.5	0.469		25.7	47.9	0.8	-1.7623	33.4216	348.8	0.362	
	50.3	43.7	0.8	-1.6347	34.3339	318.4	0.599		50.1	46.7	0.9	-1.8006	33.7238	339.0	0.417	
	74.6	43.8	0.5	-0.4641	34.514	303.9	0.688		74.3	44.8	0.8	-1.6762	33.9225	310.9	0.612	
	102	43.1	0.8	1.8051	34.7945	288.7	0.742		99.5	43.8	0.8	-1.1617	34.2593	293.0	0.692	
	125.4	43.1	0.8	2.2314	34.8603	285.7	0.762		150.7	42.4	1.2	0.1669	34.582	284.9	0.768	
	150.4	43.8	0.8	2.4824	34.9029	284.0	0.782		373	10.5	49.1	0.9	-1.7117	31.861	361.0	0.162
	200.2	43.9	0.8	2.4144	34.9207	284.1	0.8			24.2	50.9	0.8	-1.674	32.6169	359.8	0.287
279	4.7	44.5	0.7	-1.4967	32.6448	371.8	0.12	50.5		45.1	0.7	-1.7929	33.6733	334.7	0.421	
	25.5	43.5	0.8	-1.6318	33.9438	358.2	0.498	99.9		42.1	0.8	-1.396	34.1908	294.5	0.67	
	50	42.8	0.7	-0.7134	34.5466	328.3	0.659	149.8		41.3	1.3	0.071	34.5336	286.9	0.743	
	74.9	43.2	0.7	0.8505	34.7568	314.8	0.749	200.3		48.2	1.2	0.9584	34.7818	279.9	0.834	
	100.8	44.9	0.7	1.2518	34.8443	309.6	0.787	379		9.2	45.2	0.7	-1.6622	31.1065	352.0	0.152
	124.4	43.1	0.8	1.1389	34.8747	308.8	0.809			24.4	46.4	0.8	-1.6798	32.6984	348.3	0.322
	150.4	45.8	0.8	0.8942	34.8802	310.2	0.809		50.3	43.8	0.7	-1.7277	33.484	316.6	0.555	
	200.6	43.3	1.3	-0.6652	34.8056	329.2	0.738		100	41.4	0.8	-1.0232	34.2814	294.8	0.663	
250.1	44.2	0.6	-0.7638	34.8481	333.2	0.719	149.1		44.5	1.3	0.5095	34.6333	284.1	0.763		
285	9.1	43.1	0.8	-1.6248	32.5168	356.5	0.209		200.2	41.2	1.2	1.169	34.8267	279.3	0.835	
	24.3	42.8	0.8	-1.5651	33.2454	350.1	0.288		382	10.2	46.4	0.7	-1.6545	31.2707	349.6	0.142
	49.8	41.2	0.8	-0.951	34.3039	314.5	0.582			24.9	48.9	0.8	-1.669	32.6921	340.9	0.378
	75.1	42	0.8	-1.7517	34.4288	314.4	0.551	50		44.4	0.7	-1.6787	33.8547	302.0	0.582	
	100.4	43.1	1.2	-1.4458	34.4855	307.8	0.602	75.4		43.4	0.8	-1.3598	34.1941	294.1	0.66	
	200	45.6	1.2	1.1118	34.8147	292.6	0.761	100.9		43.2	1.3	-0.6064	34.3761	290.1	0.698	
	250.3	41.7	1.4	1.36	34.8696	291.5	0.794	149.7		43	1.3	0.6357	34.6692	280.7	0.798	
291	8.5	39.4	0.8	-1.6423	33.1259	364.2	0.274	200.1		42.8	1.2	1.1987	34.8316	277.3	0.881	
	24.7	40	0.8	-1.7357	34.0576	321.2	0.486	385	1	42.8	0.7	-0.9681	31.2057	345.5	0.098	
	49.7	40.2	0.7	-1.7959	34.1197	314.3	0.548		25.3	44.7	0.8	-1.6786	33.8141	332.9	0.377	
	99.3	40.6	0.7	2.1692	34.7432	283.2	0.759		49.5	43.7	0.9	-1.7919	33.9876	325.0	0.44	
	150.2	42.6	1.3	3.0943	34.9449	279.0	0.806		74.8	43	0.8	-1.4419	34.1913	303.1	0.606	
	200.6	41.1	0.8	2.9297	34.949	279.4	0.825		100.9	51.6	1.3	-0.5913	34.3882	292.4	0.679	
295	9.7	41.2	0.7	-1.6476	33.3319	347.7	0.356		150.4	43.2	1.2	1.7108	34.7925	280.1	0.807	
	29	41.1	0.7	-1.642	33.9985	341.8	0.4	200.9	43.8	0.8	2.2456	34.9106	278.8	0.837		
	50	43.6	0.9	-1.7553	34.1796	328.7	0.503	389	9.6	46.7	0.7	-0.0897	31.4661	342.2	0.233	
	114	43.2	1.2	0.817	34.5455	292.2	0.712		24	47.4	0.9	-1.6203	33.4685	334.2	0.435	
	149.9	41.1	1.2	2.7128	34.8716	279.3	0.779		50.8	44.2	0.7	-1.7382	34.023	318.1	0.483	

	199.5	43	1.3	2.8677	34.9393	279.1	0.808		76.3	43.8	0.7	-1.6317	34.2016	310.9	0.546
299	8.3	42.7	0.8	-1.6869	32.7296	346.0	0.313	400	99.8	43.9	0.8	-1.1191	34.3493	303.6	0.62
	24.2	43.8	0.9	-1.629	33.3818	344.2	0.359		149.7	43.1	1.3	1.0584	34.6955	285.8	0.754
	50.2	43.8	0.8	-1.776	34.0915	327.7	0.482		200.1	42.8	1.2	1.8562	34.8463	280.5	0.804
	74.1	42.9	0.7	-1.674	34.1898	319.5	0.551		249.7	43.5	0.7	1.928	34.8854	280.2	0.823
	100	44.1	0.8	-1.6527	34.2548	319.1	0.574		10.4	50.4	0.7	-1.5047	32.352	368.2	0.221
	200.5	41.7	0.9	1.6627	34.8274	280.0	0.821		26.8	47.5	0.7	-1.3892	33.719	323.9	0.552
301	5.6	43.7	0.8	-1.6453	33.3433	353.8	0.282	407	50.7	46.5	0.7	-1.3453	34.2078	315.1	0.627
	25.1	44.1	0.8	-1.6839	33.653	344.4	0.364		75.6	45.3	0.8	-1.5371	34.3736	321.9	0.622
	50.6	43.1	0.7	-1.8089	34.0067	327.5	0.462		101.2	45.9	1.2	-1.6239	34.417	322.8	0.635
	100.3	41.8	1.2	-0.8609	34.3054	292.3	0.676		151.2	44.3	1.2	0.0761	34.6224	309.4	0.699
	149.6	41	1.3	0.8427	34.6427	282.3	0.769		201.5	42.9	0.8	1.7387	34.8423	302.1	0.768
	200.5	42.1	0.8	1.8189	34.8386	279.3	0.821		10.1	38.8	0.7	-0.1166	29.7169	350.5	0.131
302	25	46.1	0.8	-1.6932	33.6021	346.3	0.365	411	30.3	54.9	1.1	-1.5977	33.4605	325.3	0.47
	39.6	44.8	1.8	-1.7733	33.8362	337.9	0.427		55.9	54.6	0.7	-1.6241	33.806	277.0	0.716
	47.1	45.4	0.8	-1.7774	33.9365	333.8	0.455		9.8	37.9	0.8	0.531	29.1174	350.4	0.169
	100.5	41.8	1.3	-0.8102	34.3212	293.7	0.698		14.8	50.1	0.8	1.1734	30.688	336.8	0.435
	200.5	41.8	0.9	1.4429	34.8255	281.1	0.848		20	96.6	0.7	0.4715	32.5005	309.3	0.555
306	5.3	47.5	0.7	-1.6797	32.3133	360.1	0.263	25.2	96.6	0.8	0.462	32.5024	310.5	0.533	
	24.4	45.8	0.8	-1.6919	33.4738	344.3	0.388	35.3	93.6	0.7	0.0057	32.6585	304.7	0.548	

Table 3: Parameters used in three-component and four-component mass balance following Ekwurzel et al. (2001).

	PO_4^* [$\mu\text{mol}\cdot\text{kg}^{-1}$]	$\delta^{18}O$ [‰]	Salinity
Atlantic water	0.7	0.3	34.92
River runoff	0.1	-20	0
Sea ice	0.4	surface + 2.6	4
Pacific water	2.4	-1.1	32.7

Table 4: End-member concentrations of Ba based on Guay et al. (2009).

	Ba [nM]
Atlantic water	43 ± 3
Pacific water	55 ± 5
Sea ice	5 ± 1
Eurasian runoff	$130 \pm 15 \%$
NA runoff	$520 \pm 15 \%$

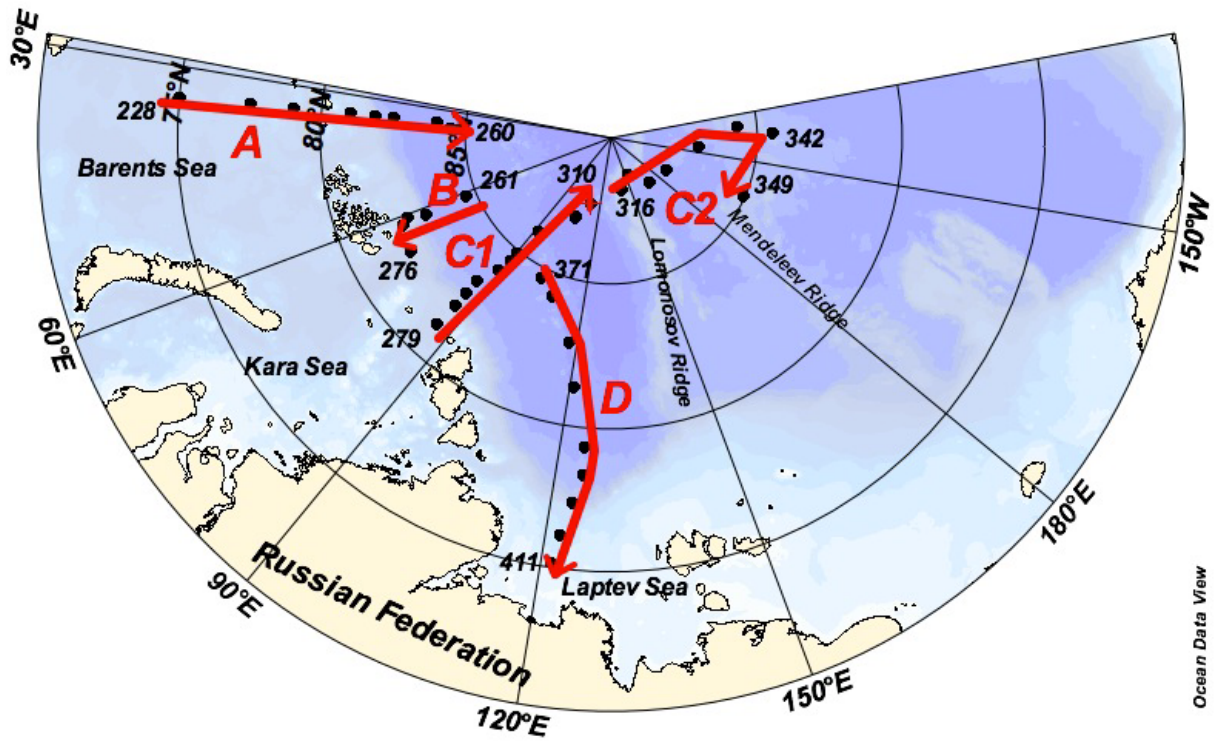


Fig. 1: Cruise map of R/V Polarstern cruise ARK-XXII/2 in 2007 (see table 1). Red arrows mark sections in the direction of travel.

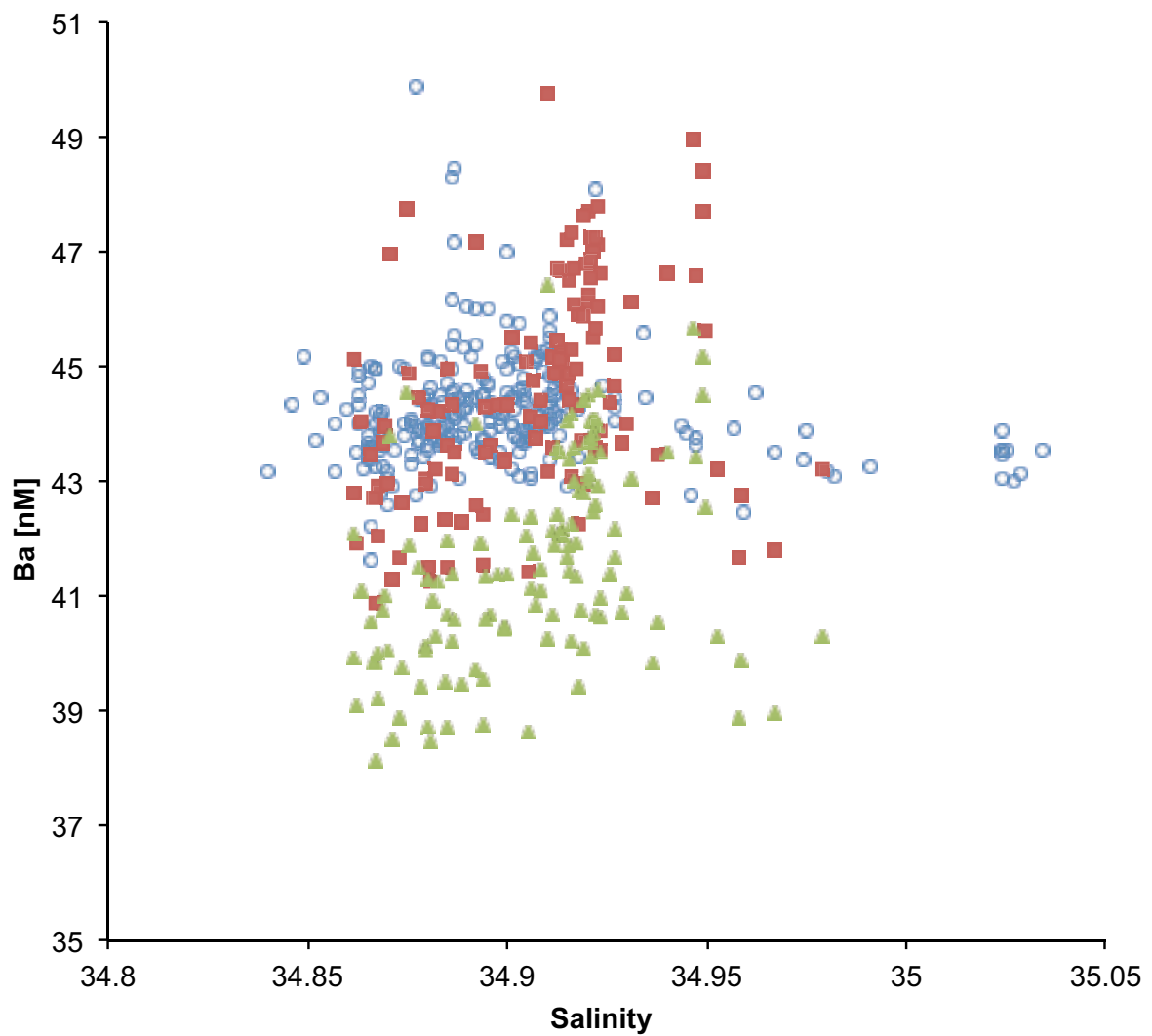


Fig. 2: Comparison of Ba/salinity systematics of all samples of salinities >34.85 of Abrahamsen and Falkner (personal communication) (blue circles) and those of our lab where we used two different standard types as absolute reference for calibrating the ^{135}Ba standard: commercial ICP MS standards (red squares) and natural waters (green triangles). Calibration with commercial standards results in 7.2 % higher absolute concentrations of dissolved Ba than calibration with natural waters and better reproduces the data from Abrahamsen et al. (2009) and previous publications on Ba in the Arctic (cf. Falkner et al., 1993; 1994; Guay and Falkner 1997; 1998).

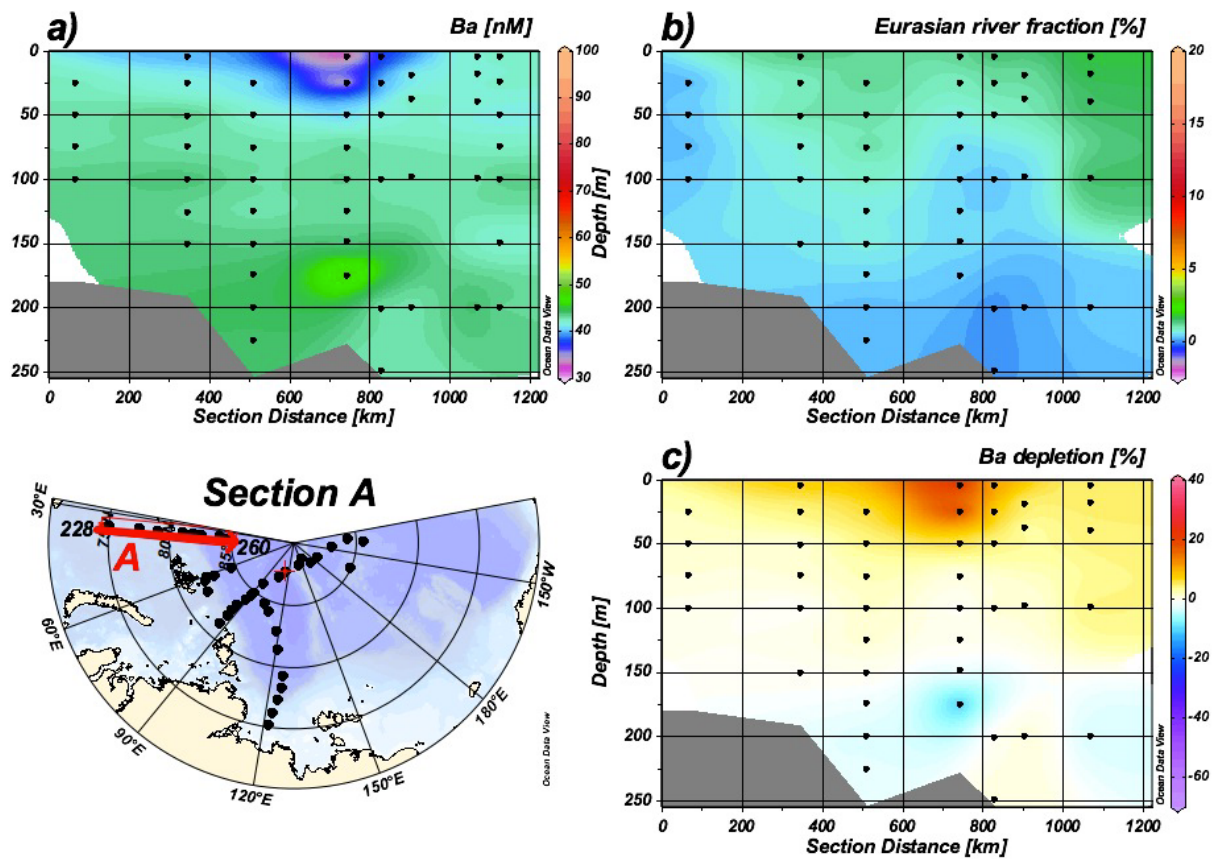


Fig. 3: Section A from the Barents Sea to the Nansen Basin: a) Concentrations of dissolved Ba [nM]; b) River water fraction [%] from the solved mass balance system matching Eurasian runoff; c) Ba depletion with positive and negative values reflecting depletion and enrichment [%] respectively. This has to be seen as a deficit or excess concentration of Ba, based on the expected concentration Ba^0 .

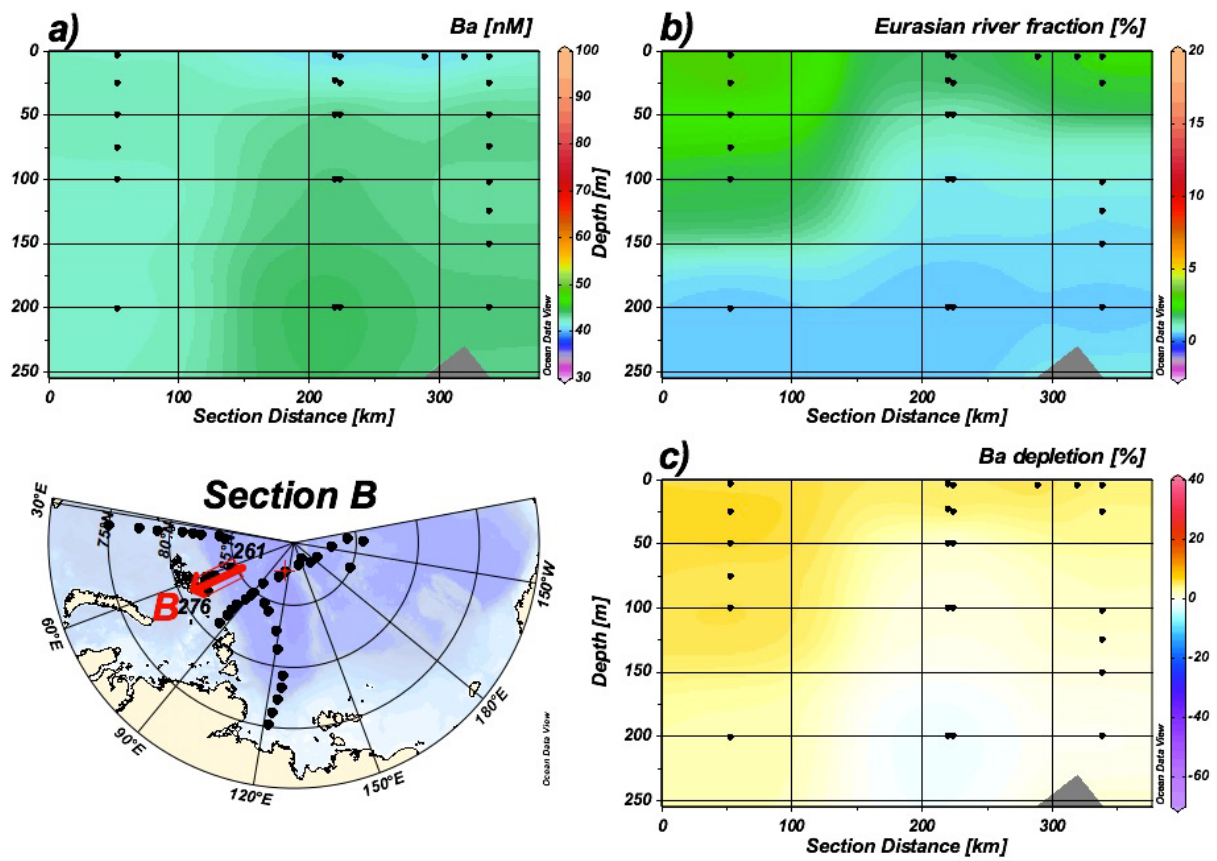


Fig. 4: Section B from the Nansen Basin to the Kara Sea slope (for details see fig. 3): a) Concentrations of dissolved Ba [nM]; b) fraction of Eurasian runoff [%]; c) Ba depletion [%].

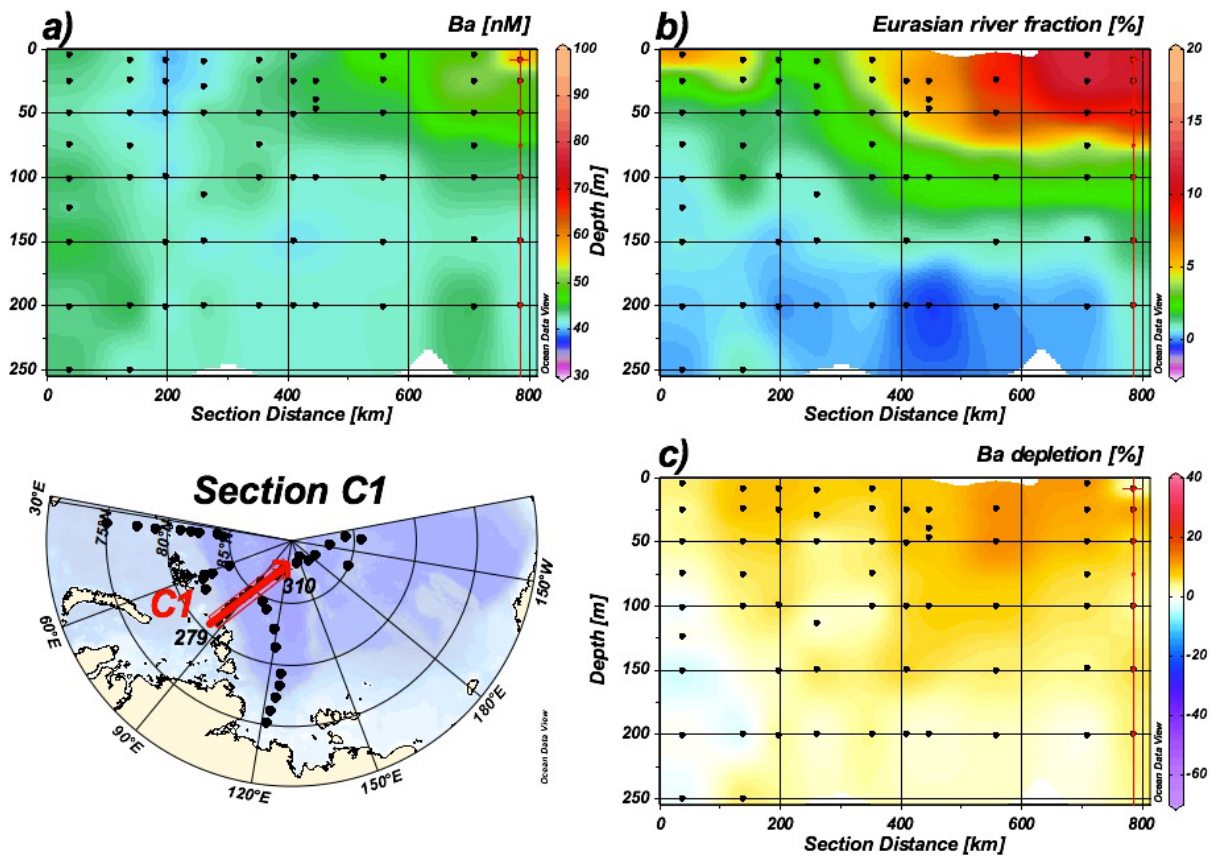


Fig. 5: Section C1 from the Kara Sea slope to the Lomonosov Ridge (for details see fig. 3): a) Concentrations of dissolved Ba [nM]; b) fraction of Eurasian runoff [%]; c) Ba depletion [%].

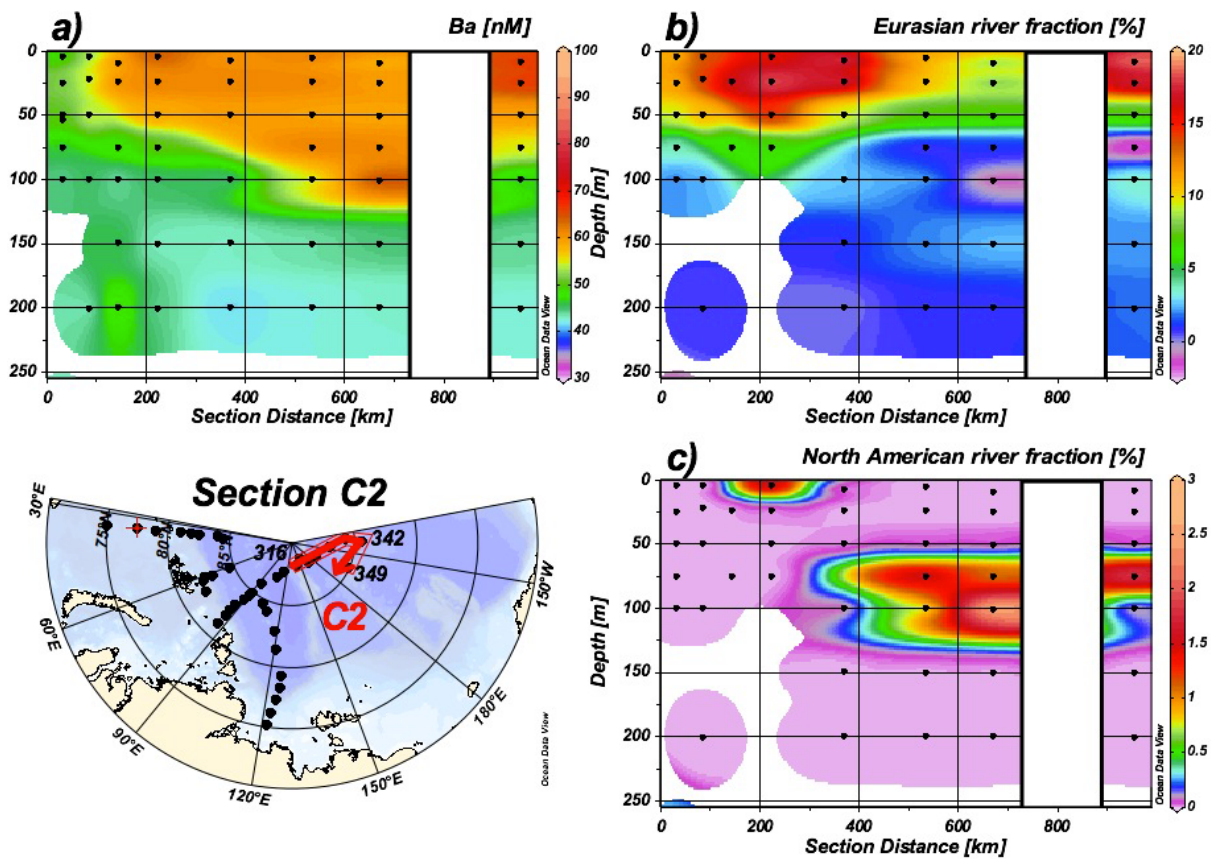


Fig. 6: Section C2 from the Lomonosov Ridge to the Alpha/ Mendeleev Ridge (for details see fig. 3): a) Concentrations of dissolved Ba [nM]; b) fraction of Eurasian runoff [%]; c) fraction of (calculated) NA runoff [%]. Panels b) and c) here assume conservative behavior of Ba. Fractions of Pacific water calculated using N/P signature.

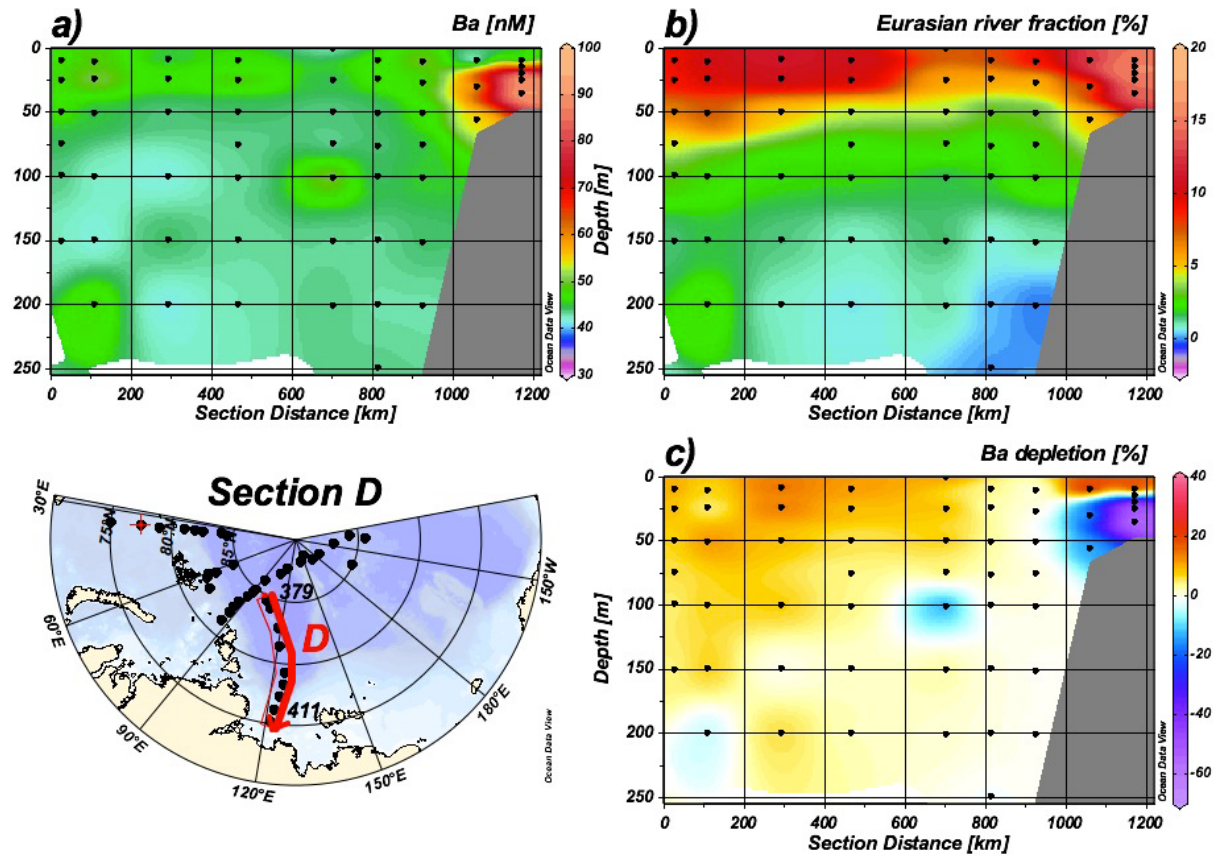


Fig. 7: Section D from the Eurasian Basin to the Laptev Sea (for details see fig. 3): a) Concentrations of dissolved Ba [nM]; b) fraction of Eurasian runoff [%]; c) Ba depletion [%].

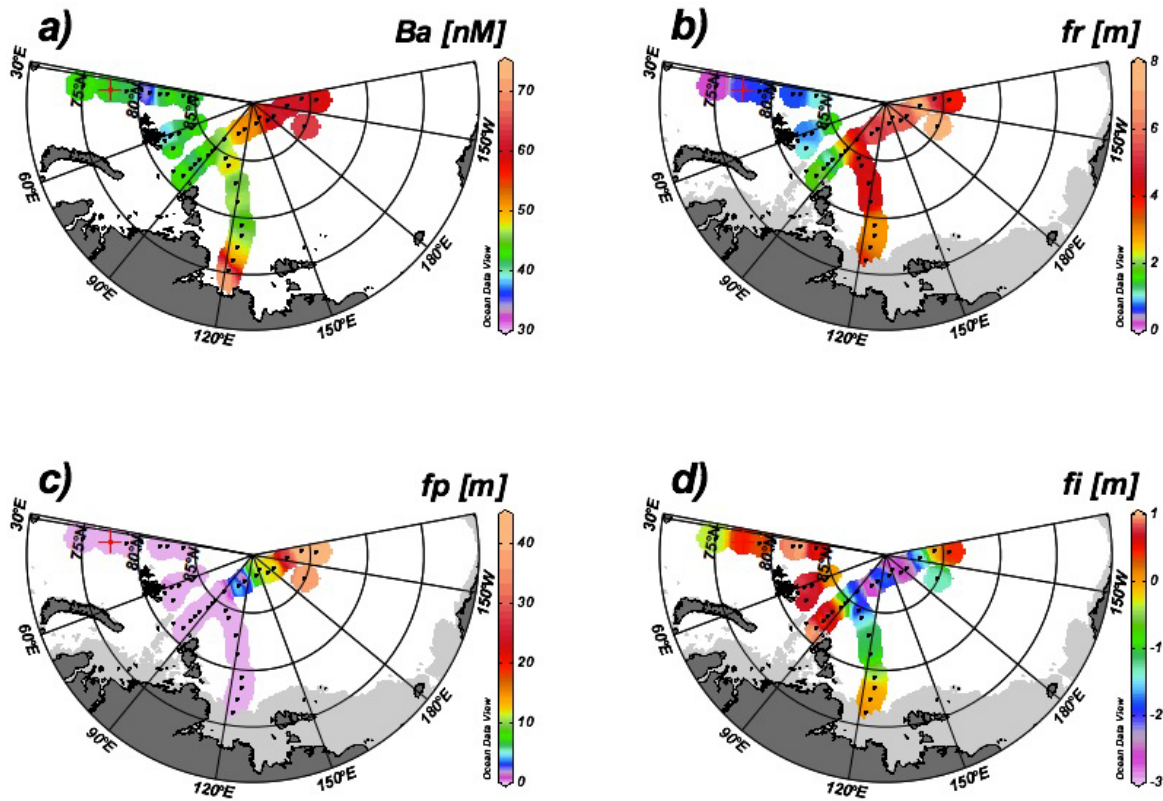


Fig. 8: Maps showing a) the average Ba concentrations in the upper 50 m, b) the integrated height [m] in the upper 50 m of river water, c) of Pacific water, and d) of sea ice melt.

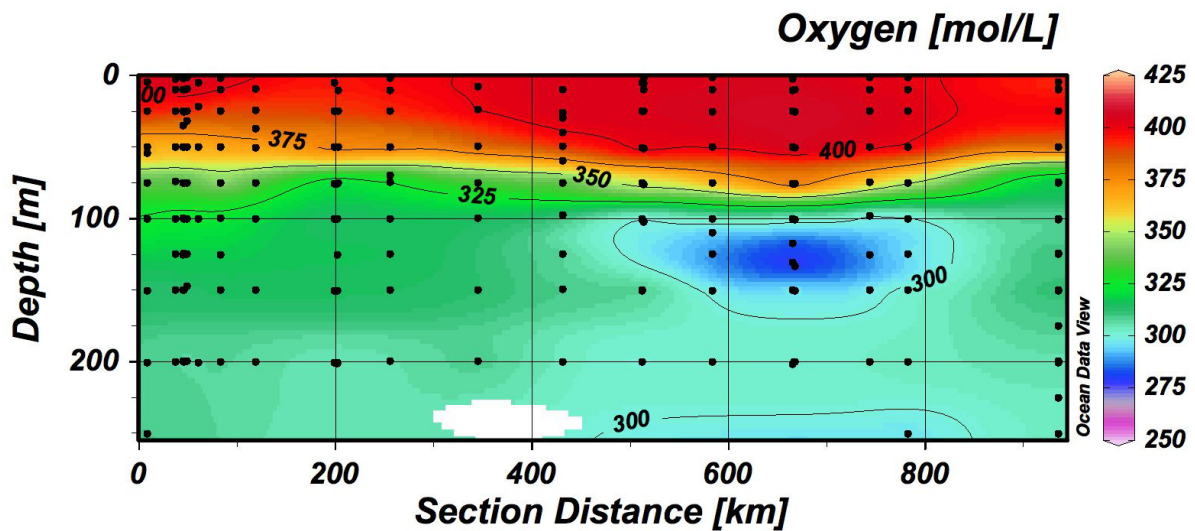


Fig. 9: Dissolved oxygen (Wisotzki, 2008) at section C2 (cf. fig. 6). An oxygen minimum is positioned at 120 m depth just below the observed maximum of Ba and silicate (cf. Middag et al., 2009).